

ON THE APPLICABILITY OF PROGRESS VARIABLE APPROACH FOR
LARGE EDDY SIMULATION OF PREMIXED FLAMES

A THESIS SUBMITTED TO
THE GRADUATE SCHOOL OF NATURAL AND APPLIED SCIENCES
OF
MIDDLE EAST TECHNICAL UNIVERSITY

BY

BULUT TEKGÜL

IN PARTIAL FULFILLMENT OF THE REQUIREMENTS
FOR
THE DEGREE OF MASTER OF SCIENCE
IN
MECHANICAL ENGINEERING

OCTOBER 2017

Approval of the thesis:

**ON THE APPLICABILITY OF PROGRESS VARIABLE APPROACH FOR
LARGE EDDY SIMULATION OF PREMIXED FLAMES**

submitted by **BULUT TEKGÜL** in partial fulfillment of the requirements for the degree of **Master of Science in Mechanical Engineering Department, Middle East Technical University** by,

Prof. Dr. Gülbin Dural Ünver
Dean, Graduate School of **Natural and Applied Sciences**

Prof. Dr. M.A. Sahir Arıkan
Head of Department, **Mechanical Engineering**

Prof. Dr. Mehmet Haluk Aksel
Supervisor, **Mechanical Engineering Department, METU**

Assist. Prof. Dr. Özgür Uğraş Baran
Co-supervisor, **Mechanical Engineering Department, TEDU**

Examining Committee Members:

Assoc. Prof. Dr. Cüneyt Sert
Mechanical Engineering Department, METU

Prof. Dr. Mehmet Haluk Aksel
Mechanical Engineering Department, METU

Assist. Prof. Dr. Özgür Uğraş Baran
Mechanical Engineering Department, TEDU

Assist. Prof. Dr. Feyza Kazanç
Mechanical Engineering Department, METU

Assist. Prof. Dr. Sıtkı Uslu
Mechanical Engineering Department, TOBB ETÜ

Date:

I hereby declare that all information in this document has been obtained and presented in accordance with academic rules and ethical conduct. I also declare that, as required by these rules and conduct, I have fully cited and referenced all material and results that are not original to this work.

Name, Last Name: BULUT TEKGÜL

Signature :

ABSTRACT

ON THE APPLICABILITY OF PROGRESS VARIABLE APPROACH FOR LARGE EDDY SIMULATION OF PREMIXED FLAMES

Tekgöl, Bulut

M.S., Department of Mechanical Engineering

Supervisor : Prof. Dr. Mehmet Haluk Aksel

Co-Supervisor : Assist. Prof. Dr. Özgür Uğraş Baran

October 2017, 79 pages

Combustion applications are the primary energy source and will continue to be for the near future. Therefore, accurate modeling of combustion applications is crucial to study and improve the processes. In this study, progress variable approach is used with the implementation of a source term found in literature to simulate selected fully premixed combustion applications. CFD computations and preprocessing steps were conducted using OpenFOAM C++ library. Thermophysical values were obtained from zero and one dimensional Cantera simulations and given as initial conditions. Obtaining flame front positions consistent with the experimental results by modeling the flame as a single scalar transport was intended. $k-\epsilon$ RANS and one-equation eddy LES turbulence models were used. Results showed that selected source term can be used independent from the application geometry or used two turbulence models. Good flame front position correlations with experimental profiles were achieved.

Keywords: Premixed flame, Combustion modeling, Progress variable, Backward facing step, Large eddy simulation

ÖZ

İLERLEME DEĞİŞKENİ METODUNUN ÖNKARIŞIMLI YANMAYA BÜYÜK GİRDAP SİMÜLASYONU İLE UYGULANMASI

Tekgöl, Bulut

Yüksek Lisans, Makina Mühendisliği Bölümü

Tez Yöneticisi : Prof. Dr. Mehmet Haluk Aksel

Ortak Tez Yöneticisi : Yrd. Doç. Dr. Özgür Uğraş Baran

Ekim 2017 , 79 sayfa

Yanma uygulamaları günümüzde birincil enerji kaynağıdır ve yakın gelecekte de bu şekilde kalmaya devam edeceği öngörülmektedir. Dolayısıyla, yanma sürecinin doğru bir şekilde modellenmesi bu uygulamaların incelenmesi ve geliştirilmesi için kritiktir. Bu çalışmada, literatürde bulunan bir kaynak terimi kullanılarak, ilerleme değişkeni metodu ile tamamen önkarişmiş yanma işlemlerinin benzetimi amaçlanmıştır. HAD hesaplamaları ve ön işleme adımları OpenFOAM C++ kütüphanesi kullanılarak gerçekleştirilmiştir. Termofiziksel değerler sıfır ve bir boyutlu Cantera benzetimlerinden elde edilip başlangıç koşulu olarak tanımlanmıştır. Alevi tek bir skaler olarak tanımlayarak deneysel verilerle örtüşen alev yüzey pozisyonlarının elde edilmesi amaçlanmıştır. Türbülans, k- ϵ RANS ve tek-denklemler Büyük Girdap Benzetimi metodu kullanılarak modellenmiştir. Sonuçlar önerilen kaynak teriminin uygulamanın geometrisi veya uygulanan iki türbülans modelinden bağımsız olarak kullanılabileceğini göster-

miřtir. Ayrıca, deneysel verilere benzerlik gösteren alev yüzeyi profilleri elde edilmiştir.

Anahtar Kelimeler: Önkariřımlı yanma, Yanma modellenmesi, İlerleme deęiřkeni, Ters basamak, Büyük girdap benzeřim yöntemi

*"Don't ever, for any reason, do anything, to anyone, for any reason, ever, no matter what, no matter where, or who, or who you are with, or where you are going, or where you've been, ever, for any reason whatsoever."
- Michael G. Scott*

ACKNOWLEDGMENTS

First of all, I would like to express my deepest gratitude to my supervisor Prof. Dr. Mehmet Haluk Aksel and co-supervisor Assist. Prof. Dr. Özgür Uğraş Baran for their help, guidance and support throughout my master studies and giving me the opportunity to pursue my goals for the rest of my career.

I would also like to thank my local advisors in Aalto University, Prof. Ville Vuorinen and D.Sc.(Tech) Ossi Kaario for giving me the chance to work on a field i am interested in and their support, encouragement and criticism throughout this thesis.

For their valuable thoughts, feedback, guidance and companionship I would like to thank Erkki, Heikki, Karri, Mahdi, Petteri and the whole Aalto University combustion research group.

I would like to express my love to my parents, Aynur and Süleyman. I owe everything I have to their efforts and dedication in raising me right. I also would like to thank my sister Yağmur for growing up to be a wonderful person and woman. In addition, I would like to thank Gülcan, Alican and Güney for being the best friends a person can ask for and their endless support throughout our friendship.

Finally, I would like to thank my girlfriend Buse for encouraging me to take risks and her full support, love and care since the day I met her.

TABLE OF CONTENTS

ABSTRACT	v
ÖZ	vii
ACKNOWLEDGMENTS	x
TABLE OF CONTENTS	xi
LIST OF TABLES	xiv
LIST OF FIGURES	xv
NOMENCLATURE	xviii
CHAPTERS	
1 INTRODUCTION	1
1.1 LES: An Emerging Approach For Premixed Combustion	1
1.2 Motivation	2
1.3 Problem Definition and Thesis Structure	4
2 PREMIXED COMBUSTION MODELING OVERVIEW	7
2.1 Overview of Different Combustion Process Types	7
2.2 Laminar Premixed Flames	9
2.3 Premixed Turbulent Combustion Regimes	11
2.4 Different Approaches for Modeling Turbulent Premixed Combustion	13

2.4.1	Detailed Chemistry Approach	14
2.4.2	Flamelet-Generated Manifold Approach	16
2.4.3	G-Equation	17
2.4.4	Progress Variable Approach	18
2.4.5	Advantages of Progress Variable Approach	20
3	METHODOLOGY	23
3.1	Governing Flow Equations	23
3.1.1	Conservation of Mass and Momentum	24
3.1.2	Energy Equation	27
3.2	Progress Variable Approach	28
3.3	Laminar Flame Speed	31
3.4	Problem Configurations	33
3.4.1	2D Bunsen Burner (RANS)	33
3.4.2	3D Bunsen Burner (LES)	36
3.4.3	Backward Facing Step	38
3.5	Numerical Methods and Boundary Conditions	40
4	RESULTS	43
4.1	2D Bunsen Burner	43
4.2	3D Bunsen Burner	49
4.3	3D Backward Facing Step	56
4.3.1	Resolution of the Case in LES Modeling	63
4.4	Discussion	66
5	CONCLUSION	69

5.1	Summary and Overview	69
5.2	Review of the Thesis Objectives	70
5.3	Future Work	71
	REFERENCES	75
	APPENDICES	

LIST OF TABLES

TABLES

Table 2.1	Species and reaction information of compared mechanisms	16
Table 3.1	Gülder correlation constants for different reactants	32
Table 3.2	Simulation parameters for $T = 300$ K	35
Table 3.3	Boundary conditions	41
Table 4.1	Comparison of nondimensionalized flame angles	48
Table 4.2	Cantera initial conditions for $p = 1$ atm $\phi = 0.57$	59
Table 4.3	Reattachment lengths for experiment and current simulation ($Re =$ 22,000)	63

LIST OF FIGURES

FIGURES

Figure 1.1	Electricity generation of Turkey from different resources	4
Figure 1.2	Estimated energy demand of Turkey for the next decade [11]	4
Figure 2.1	Combustion systems categorized by premixedness and flow type . . .	8
Figure 2.2	A schematic picture of laminar premixed flame structure [17]	9
Figure 2.3	Change of temperature and density throughout the methane flame .	10
Figure 2.4	Cantera simulation for different species in stoichiometric laminar premixed methane flame	11
Figure 2.5	Premixed turbulent flame regime Borghi diagram [19]	12
Figure 2.6	Results of different reduced mechanisms on n-dodecane combustion	15
Figure 2.7	Schematic representation of G-Equation approach [17]	18
Figure 2.8	Flamelet regions of different experimental Bunsen flames used in the thesis [37].	20
Figure 3.1	Schematic representation of progress variable approach	28
Figure 3.2	Results of different reduced mechanisms on n-dodecane combus- tion	32
Figure 3.3	Laminar flame speed for methane flame at $T = 300$ K and $p = 1$ atm	33
Figure 3.4	Computational domain for 2D Bunsen flame analysis	34

Figure 3.5	Cantera results for $\phi = 0.9$, $T_{initial} = 300$ K and $p = 0.5$ MPa	35
Figure 3.6	Computational domain for 3D bunsen burner	37
Figure 3.7	Schematic of the backward facing step problem domain [53]	38
Figure 3.8	Computational domain for backward facing step	39
Figure 4.1	Time averaged progress variable flame shape for different pressure values	44
Figure 4.2	Time averaged progress variable flame shape for different equivalence ratio values	45
Figure 4.3	Change of thermodynamic values across the flame for $\phi = 0.9$ and $p = 0.5$ MPa	46
Figure 4.4	Calculated Bunsen flame profiles with time averaged progress variable	47
Figure 4.5	Balance diagram for steady oblique flames	48
Figure 4.6	3D bunsen flames on Borghi diagram	49
Figure 4.7	Instantaneous progress variable and velocity magnitude profiles for different S_u/U configurations	51
Figure 4.8	Schematic representation of flame wrinkling [60]	52
Figure 4.9	Time averaged Karlovitz numbers for different S_u/U configurations	53
Figure 4.10	Volume rendering of instantaneous flame profile	54
Figure 4.11	Gradient of instantaneous progress variable field and instantaneous velocity profiles for different S_u/U configurations	55
Figure 4.12	Streamwise velocity profiles for cold flow	57
Figure 4.13	Time averaged profiles for streamwise velocity component at different cross sections for non-reacting flow	58

Figure 4.14 Time averaged profiles for streamwise velocity fluctuations at different cross sections for non-reacting flow	58
Figure 4.15 Instantaneous progress variable profiles for $t = 0$ to $t = 0.5$ s	59
Figure 4.16 Thermodynamic parameters and progress variable fields	60
Figure 4.17 Schlieren photograph of the reactive flow [53]	61
Figure 4.18 Time averaged progress variable field	61
Figure 4.19 Gradient of time averaged progress variable field	61
Figure 4.20 Time averaged profiles for progress variable values at different cross sections for reacting flow	62
Figure 4.21 Streamlines for cold flow	63
Figure 4.22 Streamlines for reactive flow	63
Figure 4.23 Kolmogorov and integral length scale contours	65
Figure 5.1 Review table for performed simulations	73

NOMENCLATURE

u'	Turbulence intensity
s_L, S_u	Laminar Flame Speed
S_t	Turbulent Flame Speed
l	Turbulence length scale
l_F, l_Y	Flame thickness
Re	Reynolds number
Re_t	Turbulent Reynolds number
Ka	Karlovitz number
τ_c	Chemical time scale
τ_k	Turbulent time scale
ρ	Density
p	Pressure
R	Universal gas constant
T	Temperature
Y_i	Mass fraction of species i
w_i	Species source term
w_T	Energy source term
w_c	Progress variable source term
t	Time
κ	Curvature effect
D_K	Diffusion coefficient
c	Progress variable
b	Regress variable (1-c)
V	Velocity vector
μ	Dynamic viscosity
ν	Kinematic viscosity
σ_{ij}	Stress tensor
$G(x)$	Filtering kernel
S_{ij}	Strain-rate tensor
ν_t	Sub-grid scale viscosity
k	Turbulent kinetic energy
ε	Turbulent dissipation

Δ	Filtering length
C_s, C_μ	LES model constants
Sc	Schmidt number
I_0	Stretch factor
Σ	Flame surface density
ν	Kinematic viscosity
μ	Absolute viscosity
Ξ	Turbulent-laminar flame speed ratio
Le	Lewis number
ϕ	Equivalence ratio
y^+	Dimensionless wall distance
u_0	Mean inlet velocity

CHAPTER 1

INTRODUCTION

Combustion applications have been the primary energy source from households to big industrial applications. At present, combustion takes up about 90% of the worldwide energy generation, which makes it an important field of study [1]. During the past, many experimental studies were conducted to improve and increase the efficiency of combustion applications. With the advancements in computing technologies, analysis that could only be performed with sophisticated experimental tools twenty years ago now can be modeled and simulated with computers. Although this does not mean that experimental analysis has become obsolete, it can be deduced that numerical analysis of combustion has gained importance with the scientific and computational advancements.

1.1 LES: An Emerging Approach For Premixed Combustion

In the last twenty years, Large Eddy Simulation (LES) has become a major tool for simulating non-reacting flows due to the increase in available computational power [2]. This increase has enabled researchers and engineers to successfully resolve the majority of turbulent scales, while modeling the sub-grid scales through various turbulence models. The level of detail achieved by LES gives more detailed results compared to the RANS methods. For instance, Pitsch [3] stated that LES clearly have more advantages over than the RANS methods for resolving smallest scales in both premixed and non-premixed turbulent combustion simulations. In addition, Mahesh *et al.* [4] performed reactive LES analysis on complex geometries such as Pratt & Whitney premixed gas turbine combustor and reported good correlation with the ex-

perimental engine data. However, several problems still remain unresolved regarding LES applications on reacting flows. For example, in premixed combustion applications, chemical reactions usually occur in a thin flamelet region that is smaller than the computational grid used in LES, thus making the combustion chemistry inside the flame hard to resolve by conventional LES methods. Studies on the experimental and numerical analysis of laminar flames reported a thermal flame thickness of the order 10^{-4} m [5–8]. Capturing the small chemical scales in such configuration would require a filter length in the order of 10^{-5} to 10^{-6} m, which increases the already high computational cost of LES simulations. This problem has created the need for an accurate modeling of sub-grid scale combustion physics in order to simulate combustion with less computational requirements. Therefore, different approaches for combustion modeling have been developed.

A simpler approach divides the problem domain into completely burnt and unburnt regions and considers the flame as a thin interface between them. In addition, chemical reactions within the flame are modeled algebraically instead of solving species transport equation for all species involved. This method is usually referred to as flame surface density, or progress variable approach. It has proved itself to be valid for a wide variety of premixed combustion configurations. To be able to obtain information on flame kinetics with relatively low computational cost, this thesis aims to implement and evaluate the performance of a flame-wrinkling progress variable approach and rate closure equation with LES modeling using the open source CFD library OpenFOAM and the Cantera software, a tool for solving problems involving chemical kinetics, thermodynamics and transport processes.

1.2 Motivation

For the past century, the energy need in both industry and daily usage has been exponentially increasing globally [9]. With the advances in industrial applications and transportation technologies, combined with the increase in population, this trend is expected to continue in the foreseeable future. Although new technologies and applications have been utilized in renewable energy field for the past several decades, conventional energy production methods still remain as the primary source of the en-

ergy. For example, Figure 1.1 and 1.2 show the energy sources used in Turkey's electricity generation and the predicted energy demand for the following years [10, 11]. In Figure 1.2, the legend stands for names of different deep learning algorithms used in the estimation calculations. It can be seen that the energy source has heavily depended on coal and natural gas for the past several decades. Although increasing efforts have been made for finding alternative clean energy solutions, some aspects of it still remain problematic such as efficiency and the initial cost of the systems. Therefore, conventional methods still cover the major percentage of energy generation. In addition, studies also show that NO_x and CO_2 emissions caused by the combustion processes are hazardous for human health and environment [12]. With the ongoing global warming threat affecting the whole planet, optimization of conventional combustion energy production methods has become a primary concern.

Recently, International Maritime Organization (IMO) announced new regulations for much lower sulphur emissions from marine vessels visiting EU ports, which will take effect starting from 2020 [13]. New regulations limiting NO_x emissions in similar manner is expected by the end of 2030. To be able to comply these new requirements, major engine companies are seeking new ways to reduce the gas emissions while keeping the engine efficiency within an acceptable limit. Having strong ties to Finnish industry companies such as Wärtsilä, VTT and many other EU companies, Thermodynamics and Combustion Research Group in Aalto University have been working on this problem with academic and industrial funding for some time.

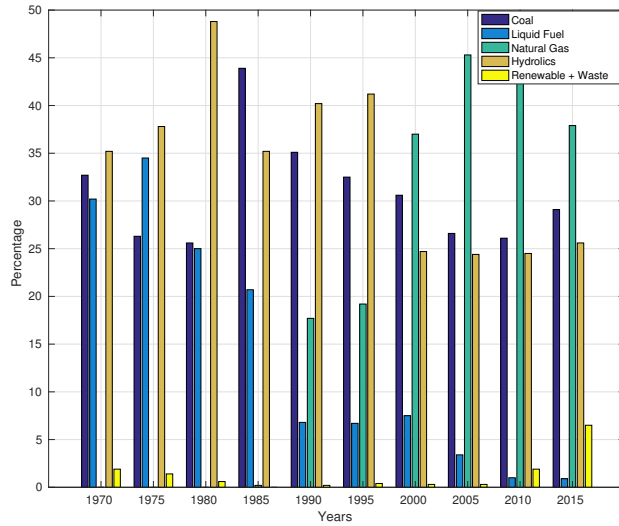


Figure 1.1: Electricity generation of Turkey from different resources

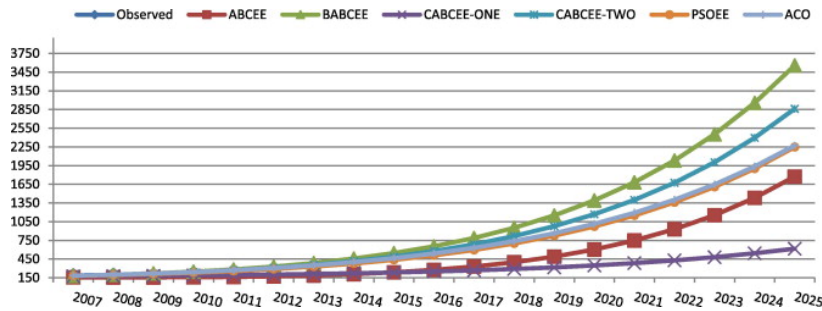


Figure 1.2: Estimated energy demand of Turkey for the next decade [11]

1.3 Problem Definition and Thesis Structure

Combustion occurs as a result of chemical reaction between fuel and oxidizer. All the chemical reactions take place in a thin region called the flame, which makes conventional CFD methods inefficient to capture as well as completely resolve the chemical and flow structures in this region. The constant increase in the available computational power enables combustion modeling to be studied in more detail compared to past. However, modeling a multi-physical phenomena such as combustion without any models or simplifications still requires a lot of computational resources. Therefore, different and simpler approaches have been investigated and considered to be

used in combustion simulations of industrial applications. There are different modeling approaches available for combustion processes and each model has its advantage and drawbacks. The previous literature has shown that in contrast to detailed modeling of combustion chemistry, progress variable approach is an inexpensive solution to capture flame characteristics and position. Poinso [14] stated that using more complete chemical reaction descriptions and reaction species requires accurate modeling of thermodynamics, transport coefficients, conductivity and diffusion, which typically increases computational requirements by one order. Furthermore, comparative studies conducted by Ma *et al.* [15] and Duwig [16] showed that if the source term modeling is handled properly, progress variable approach is a fast and powerful tool for getting crucial information on premixed combustion characteristics of combustor systems. Although progress variable gives less detailed results compared to other approaches discussed in the next chapter, it still can be considered as a good compromise since less resources are required. However, it should be noted that progress variable approach requires fine-tuned case setups, well created computational grids and numerically and empirically verified modeling terms, which makes this approach a suitable tool to utilize for combustion simulations. Nevertheless, when it is optimized to a specific case, the computational power required to obtain a meaningful solution is much smaller than other methods. Hence, simplified models such as progress variable approach gains importance.

This thesis focuses on the application of the progress variable approach to different premixed combustion configurations. Structure of this thesis is as follows:

- Implementation of an existing source term reaction closure equation from literature to the OpenFOAM open source progress variable solver for premixed combustion
- 2D Bunsen burner flame analysis with the RANS turbulence model and comparison with experimental results
- 3D LES Bunsen burner analysis to assess the performance of the model on capturing accurate flame position and wrinkling behavior
- 3D backward facing step simulation to show the performance of the model in the turbulent reactive flow

Although this thesis focuses on modeling relatively simple cases compared to industrial applications, it aims to lay the foundation for improved premixed combustion modeling techniques, which would be useful in analyzing and understanding industrial applications such as IC engines. Validating the performance of progress variable approach on the selected cases may not guarantee its applicability to complex real life situations. However, this validation in more stable regimes such as Bunsen flames can provide information for its applicability for more complex problems. Results and findings of this thesis will provide a background on more complex future studies on engine combustion.

CHAPTER 2

PREMIXED COMBUSTION MODELING OVERVIEW

In most real life combustion applications, flow characteristics are turbulent. In addition, chemical processes occur during combustion are affected from turbulent flow behavior. Therefore, successful modeling of turbulent combustion by taking chemical and sub-grid scale effects into consideration has to be carefully accounted for [15]. In Section 2.1, information on different combustion process types are presented. Section 2.2 and 2.3 give information on laminar and turbulent premixed flames and different combustion regimes based on flow characteristics. Finally, Section 2.4 provides key concepts of premixed combustion modeling with progress variable approach and other different methods.

2.1 Overview of Different Combustion Process Types

Combustion processes can be classified by their specific characteristics. There are two main types of combustion processes: premixed and non-premixed combustion. In premixed combustion, fuel and oxidizer are completely mixed on the molecular level before the reaction starts to occur. Due to this prior mixing, the whole process occurs faster and even more efficient in some cases. In premixed combustion control over the process is much easier. For example, mixture can be formed in lean conditions to avoid high temperatures, thus low levels of pollutant formation is achieved. However, the reaction process is quite unstable since the reactants are already mixed and ready to react. Eventually, the flame can propagate inside the fuel source and damage the combustor system, which is defined as flashback.

In non-premixed combustion, fuel and oxidizer are separate from each other and

mixing of the reactants occurs simultaneously with burning process. A typical example for this type of combustion is furnaces. Despite the need for mixing during combustion process, non-premixed combustion is much safer compared to premixed combustion. Hence, such a combustion type could be preferred when safety of the system is the main concern. Diesel engines and gas turbines are some applications of non-premixed combustion. Furthermore, aircraft gas turbine engines are operated with non-premixed combustion processes, since safety is the primary concern in aeronautical applications. Figure 2.1 presents different combustion types and real life application examples.

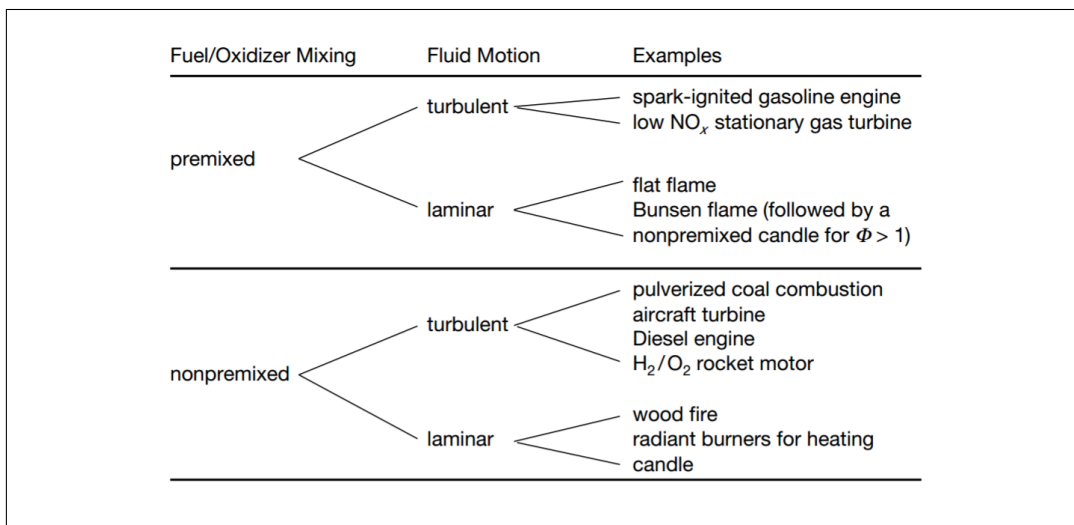


Figure 2.1: Combustion systems categorized by premixedness and flow type [1]

Premixed and non-premixed combustion has different physical characteristics. Therefore, models developed for turbulent combustion processes usually focus on only one type of combustion process. This thesis focuses on perfectly premixed combustion, since progress variable approach is only applicable in premixed combustion. Numerical models and test cases throughout this thesis are chosen based on the premixed combustion method properties.

2.2 Laminar Premixed Flames

In premixed flames, fuel and oxidizer mix homogeneously prior to combustion. When a heat source in the form of ignition is supplied, a flame is formed which propagates through this mixture. Although most combustion applications occur in turbulent regimes, it is important to investigate the laminar premixed flames first to comprehend the thermophysics of this type of combustion independent from turbulence effects.

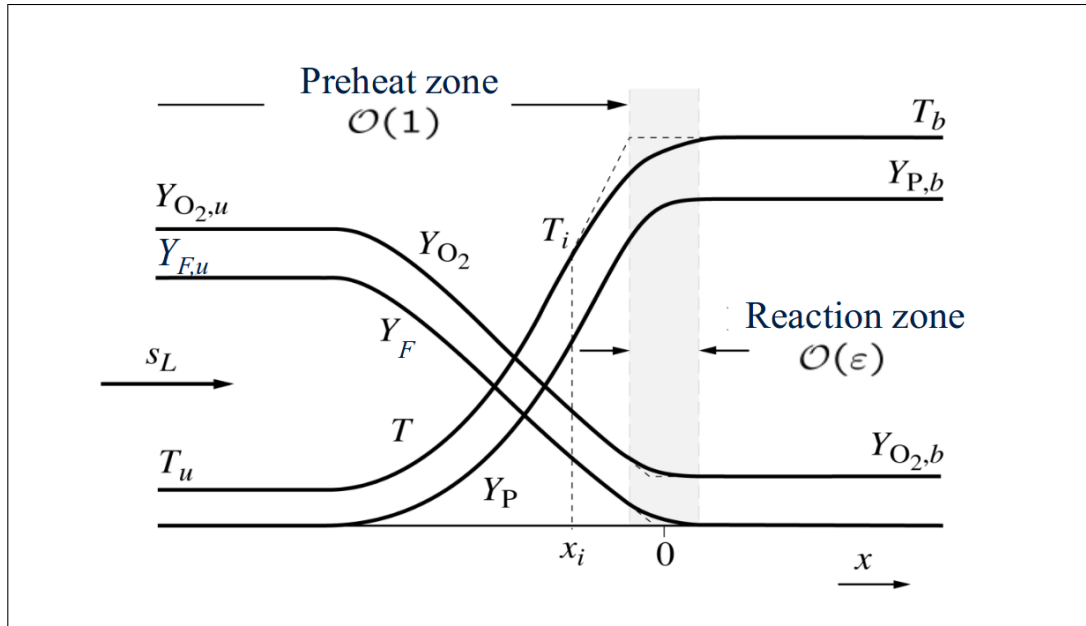


Figure 2.2: A schematic picture of laminar premixed flame structure [17]

In Figure 2.2, a schematic for premixed laminar flame structure is presented [17]. Three main layers are present in the laminar premixed flame. As seen in the figure, the left side of the domain is called the preheat zone. This layer has low reaction rates and contains unburnt fresh gases. Temperature increases to a certain limit in this region in order to make the transition of the mixture to the next layer easier. The flame layer (or reaction zone) is the layer with high rate of chemical reactions. In this region, burning of fuel to products occurs and the temperature increases exponentially. The flame progresses with a finite speed and thickness. Flame layer is what separates burnt gases from unburnt gases in the premixed mixture. Although not mentioned in Figure 2.2, the right side of the flame is defined as the oxidation layer. In this region,

radicals formed at the flame layer are completely oxidized and burning process is finalized. In addition, Figure 2.3 illustrates the transition from the unburnt state to burnt state, which shows the inverse behavior of temperature and density through the flame. Using the ideal gas law, it can be deduced that the pressure of the gas remains almost constant throughout the flow.

To illustrate the regions of the laminar flame, 1D methane combustion simulations are performed in Cantera and the resulting mass fraction plots are presented in Figure 2.4a. The reactant CH_4 starts to deplete in the reaction zone, while the mass fraction of the end product CO_2 increases. Formation of intermediate species such as CH_2O can be seen as well, in the reaction layer. If the region around reaction layer is examined in more detail, it can be observed that the formation of CO_2 starts before OH formation. OH formation is an indication of high gradients in temperature, which means that where flame rests. Therefore, region with CO_2 formation with no OH present can be defined as the preheat zone. A plot focusing on the reaction zone is presented in Figure 2.4b.

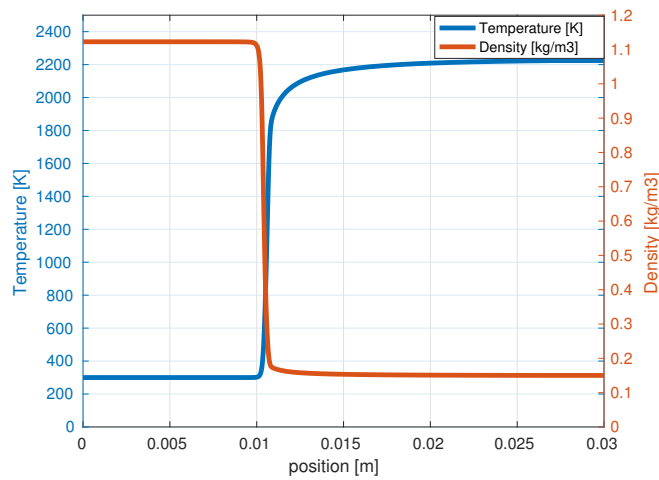


Figure 2.3: Change of temperature and density throughout the methane flame

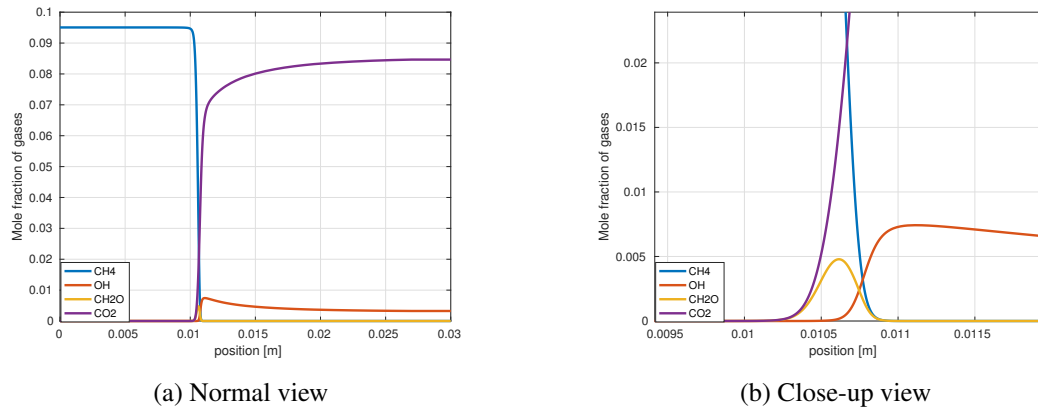


Figure 2.4: Cantera simulation for different species in stoichiometric laminar premixed methane flame

Due to the complexity in the chemical process during combustion, laminar flame regime is the most suitable region for studying flames before moving into more complex cases. In laminar region, there are no turbulent flow characteristics affecting the flame. Therefore, thermophysical properties of combustion can be studied more easily. Findings of this region can later be extended to turbulence driven regimes.

2.3 Premixed Turbulent Combustion Regimes

There are different approaches for simulating premixed turbulent flames. One approach proposes that the reaction zone of the flame lies on thin propagating surfaces, which consists of laminar flamelets added to each other. This approach is named as laminar flamelets approach [18]. According to the effect of turbulence on combustion, turbulent flames can be categorized into different regimes in laminar flamelet approach. One representation available for these different regimes is called Borghi Diagram. An improved version of Borghi Diagram is developed by Peters [19] and given in Figure 2.5.

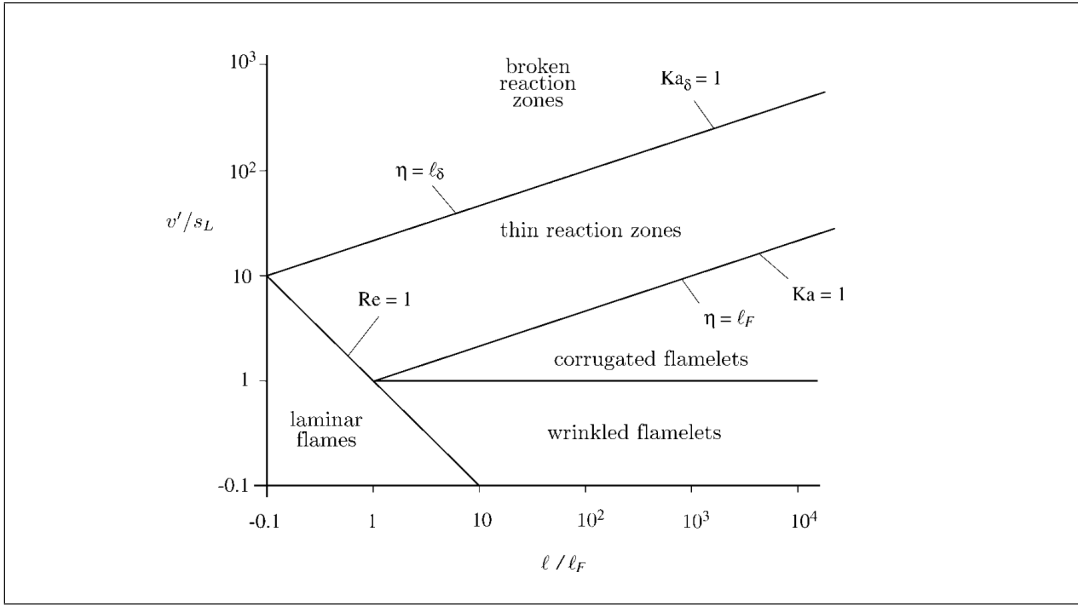


Figure 2.5: Premixed turbulent flame regime Borghi diagram [19]

In the figure, u' , s_L , l_F , l , Re and Ka are turbulence intensity, laminar flame speed, flame thickness, turbulent length scale, turbulent Reynolds number and Karlovitz number, respectively. While the x-axis is the ratio of turbulent length scale to flame thickness, y-axis of the Borghi diagram is governed by turbulence intensity to laminar flame speed.

Karlovitz number is a dimensionless number used in turbulent combustion and equals to the ratio of chemical time scale τ_c to Kolmogorov turbulent time scale τ_k :

$$Ka = \frac{\tau_c}{\tau_k} \quad (2.1)$$

For cases where Karlovitz number is less than 1, chemical reactions dominate over turbulent scales and turbulence cannot affect the internal structure of the flame, where chemical reactions take place [20]. Turbulent Reynolds number is defined as:

$$Re_t = \frac{u' l}{s_L l_F} \quad (2.2)$$

Following explanations can be made for these regions of the diagram:

- Laminar Flame Region : For $Re < 1$, the flame is completely laminar and turbulence has no effect on the flame shape or chemistry.
- Wrinkled Flamelet Region : In this region, u' is much smaller than s_L , which results in eddies with large enough turnover velocity to wrinkle the flame front. Still, turbulent structures has no effect on the chemical structures inside the flame. Laminar propagation dominates over small turbulent effects and corrugations within the flame structure are smoothed as the flame propagates.
- Corrugated Flamelet Region : In this regime, $Re > 1$ and $Ka < 1$. This means although the flame structure is perturbed by turbulent eddies externally, inner structure of the flames is confined inside the Kolmogorov scale eddies in quasi-laminar state. In addition, chemical reaction zone within the flame is not perturbed by turbulent scales.
- Thin Reaction Zone : This region is separated from corrugated flame region by $Ka = 1$ condition, where flame thickness and Kolmogorov length scale are the same. In the thin reaction zone, smallest eddies at the Kolmogorov length scale can enter inside the reacting region in the flame structure.
- Broken Reaction Zones: In this region, small eddies can easily penetrate into the reaction zone of the flame. This makes it impossible to use laminar flamelet assumption when modeling turbulent flame.

2.4 Different Approaches for Modeling Turbulent Premixed Combustion

Simulating turbulent premixed flames is a challenging task due to the turbulent characteristics of the flow and complexity of chemical reaction processes. Although mass and momentum conservation equations along with turbulence modeling is sufficient for solving a simple fluid flow case, additional thermodynamic relations such as species and energy equations must be utilized for flame and combustion calculation. Combustion is a complex physical process where reactants exothermically react with each other and form different intermediate species before forming products. In order to capture the full physical combustion process, mass, momentum and energy equations coupled with the equation of state should be solved together. Since com-

bustion process involves different species, transport equation for each species should also be added. A set of filtered equations that need to be solved during a combustion simulation can be written as follows [16]:

$$\begin{aligned}
\frac{\partial \bar{\rho}}{\partial t} + \nabla \cdot (\bar{\rho} \tilde{u}) &= 0 \\
\frac{\partial \bar{\rho} \tilde{u}}{\partial t} + \nabla \cdot (\bar{\rho} \tilde{u} \tilde{u}) &= -\nabla \bar{P} + \nabla \cdot (\bar{\rho} \tilde{u} \tilde{u} - \overline{\rho u u} + \mu \nabla \tilde{u}) \\
\frac{\partial \bar{\rho} \tilde{Y}_i}{\partial t} + \nabla \cdot (\bar{\rho} \tilde{u} \tilde{Y}_i) &= \nabla \cdot (\bar{\rho} \tilde{u} \tilde{Y}_i - \overline{\rho u Y_i} + \rho D_i \nabla \tilde{Y}_i) + \bar{w}_i \\
\frac{\partial \bar{\rho} \tilde{T}}{\partial t} + \nabla \cdot (\bar{\rho} \tilde{u} \tilde{T}) &= \nabla \cdot (\bar{\rho} \tilde{u} \tilde{T} - \overline{\rho u T} + \rho D_T \nabla \tilde{T}) + \bar{w}_T \\
\bar{\rho} &= \left(\frac{P}{RT} \right)
\end{aligned} \tag{2.3}$$

The equations presented above are the conservation of mass, conservation of momentum, conservation of each species mass fraction in the mixture, conservation of energy and ideal gas equation, respectively. w_i and w_T terms in these equations are reaction source terms for species and energy. The bar operation symbolizes filtering and $\tilde{\cdot}$ represents the density weighted averaging.

The governing reactive flow equations constitute a set of computationally stiff equations, which are challenging to solve without some simplifications. The number of species involved in combustion is high. In addition, source terms are making the ODE system too stiff for obtaining numerical solution. To overcome this problem, different modeling methods of species and source terms have been developed.

2.4.1 Detailed Chemistry Approach

The most accurate and in depth method for simulating combustion processes is direct chemistry method. Direct chemistry method uses chemical mechanisms containing the main and intermediate species involved in the combustion process along with their chemical and thermodynamic properties. This method solves the time-dependent transport equations for species involved in combustion along with mass, momentum and energy conservation equations, which are needed for viscous compressible flows. Chemical mechanisms, which govern the species and reactions involved in the pro-

cess, are used to determine which intermediate species and reactions are to be taken into account during simulation. Although there are *reduced* mechanisms consisting of smaller number of species and reactions, most of the mechanisms are really detailed. By solving these equations, information on thermodynamic and chemical state of the system is obtained. However, even with the increased computational power available, these kind of detailed simulations of simple combustion configurations would take days, even weeks to give results. Therefore, applying this methodology to real systems, such as furnaces or gas turbines, would not be feasible in the foreseeable future.

As shown in Figure 2.6, a study conducted by Masouleh *et al.* [21] considers 5 different chemical mechanisms and gives comparative results on their performances with the Cantera software through 1D simulations. Information on chemical mechanisms used in this study can be found in Table 2.1.

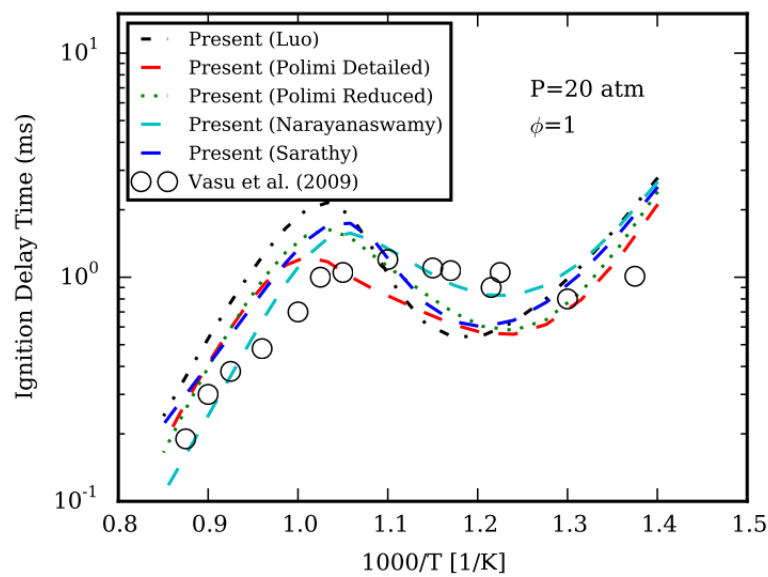


Figure 2.6: Results of different reduced mechanisms on n-dodecane combustion [21]

Table2.1: Species and reaction information of compared mechanisms

Mechanism Name	Species	Reactions
Sarathy [22]	2,755	17,460
Polimi Detailed [23]	451	17,848
Narayanaswamy [24]	255	1,512
Polimi Reduced [25]	130	2,323
Luo [26]	105	726

Different approaches have been implemented in order to reduce the computational cost of combustion simulations. One of the earliest attempts was to reduce the chemical reaction to a few global reactions and simplify the intermediate formation process between cold reactants and hot products. However, inaccuracy of this simplification makes it harder to use this method in simulations of real life applications.

2.4.2 Flamelet-Generated Manifold Approach

Another developed method focuses on laminar flamelet approach and solves the chemistry side of the combustion using pre-compiled flamelet look-up tables. Since laminar flamelet approach considers the multi-dimensional flames as an assembly of laminar flamelets, chemical compositions of these laminar flamelets will be close to that of 1D laminar flames. Using this idea, 1D flamelet equations are solved for different controlling variables such as enthalpy and stored in a look-up table to be used in run-time calculations. By replacing the specie equations with controlling variables, information of species are stored in a database. A manifold is constructed using this chemical database containing 1D chemical reaction data. This flamelet look-up table then can be used in 2D, even 3D calculations. This method is referred as Flamelet-Generated Manifold (FGM) [27]. It uses chemical mechanisms such as Gas Research Institute Mechanism (GRI-Mech), which consists of optimized chemical reaction look up tables to calculate thermodynamic and chemical properties of combustion processes [28]. These *reduced* mechanisms take the key intermediate reactions into account rather than solving for every single step in the reaction. Van Oijen and De Goey [27] first derived the flamelet equations for manifold creation and validated the approach by comparing it with burner stabilized flame results. In

addition, Fancello [29] simulated different laminar and turbulent combustion configurations using this approach and reported satisfactory results for simple fuels such as methane. Finally, Wehrfritz *et al.* [30] studied the target conditions of a more complex diesel surrogate n-dodecane fuel using this approach. They reported that the manifolds formed by reduced chemical mechanisms were able to capture the Ignition Delay Time (IDT) trends of the spray experiments correctly.

2.4.3 G-Equation

Although the detailed chemistry and FGM methods are computationally expensive, they have proven to be suitable approaches for combustion simulations. However, this thesis focuses on approaches confining species and energy equations into a single scalar transport equation, hence simplifying the calculations extremely [16]. For premixed combustion, these models are either based on progress variable approach or G equation formulation [17]. G equation formulation assigns a scalar value greater than zero for unburned area and less than zero for burned area. Then, a transport equation is solved in order to determine the flame front, which lies at the $G = 0$ iso surface [17, 31]. Finally, the flame front is tracked by calculating the relative position of each cell as positive or negative from the $G = 0$ isoline and locating the flame position. Transport equation for G, which is applicable in corrugated and thin reaction regimes, is defined as

$$\rho \frac{\partial G}{\partial t} + \rho u \cdot \nabla G = \rho s_L |\nabla G| - \rho D_\kappa |\nabla G| \quad (2.4)$$

where t , ρ , u , κ and s_L are time, density, velocity, curvature effect and laminar flame speed respectively [32]. In Figure 2.7, schematic representation of G-Equation approach is presented.

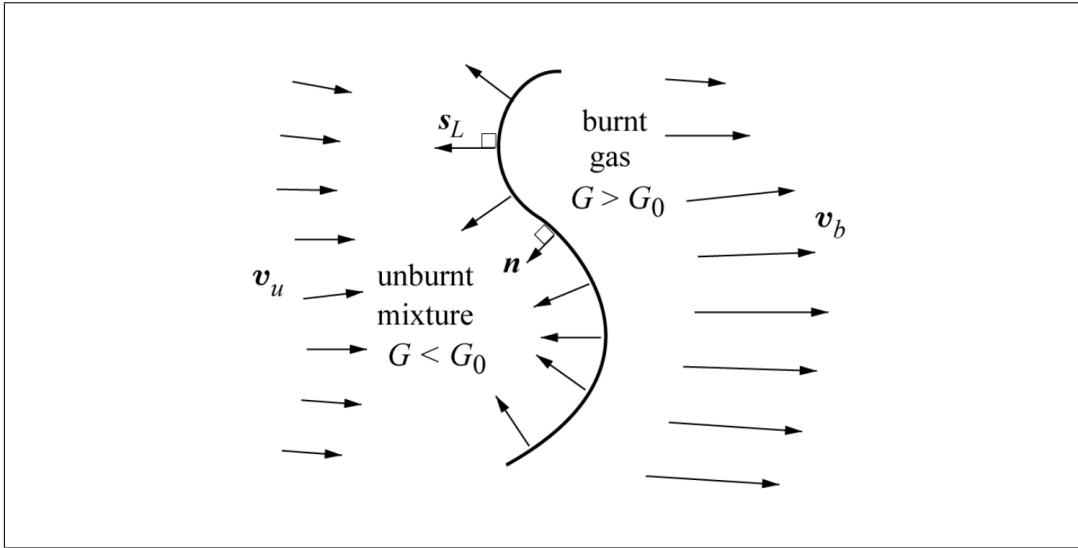


Figure 2.7: Schematic representation of G-Equation approach [17]

Pitsch contributed to the formulation of this approach on premixed turbulent combustion applications, and also conducted validation and benchmarking studies with De Lageneste to verify the applicability of the model [33, 34].

2.4.4 Progress Variable Approach

The main focus of this thesis is the progress variable approach. In progress variable approach, the set of equations needed to be solved in Equation 2.3 is simplified by defining a scalar c from normalized temperature or fuel mass fraction. By doing so, instead of representing the flame through energy and species transport equations, it is reduced to a single scalar transport equation as seen in Equation 2.5 [35].

$$\tilde{c} = \frac{\tilde{Y}_F - Y_{F_u}}{\tilde{Y}_{F_b} - Y_{F_u}} = \frac{\tilde{T} - T_u}{T_b - T_u} \quad (2.5)$$

In Equation 2.5, Y is mass fraction, T is temperature with subscripts u and b representing burned and unburned. In this approach, chemical reactions are completely neglected and the flame behavior is reduced to a single scalar through a transport equation. Lin [36] utilized this method for simulating both 2D and 3D turbulent

freely propagating flames, along with 3D turbulent Bunsen flames using LES. He observed accurate LES predictions for turbulent cases with $u'/s_L < 6-8$ region. In addition, Muppala *et al.* [37] used progress variable approach with RANS turbulence model. They modeled the reaction rate term by using a fitting function for experimental Bunsen flame data and obtained good results. Later, this work has extended to LES turbulent model and proved to be valid for similar cases [38].

By using progress variable approach method, Shahbazian [39] implemented different algebraic and transport source term models and compared their performance on a premixed turbulent Bunsen type flame configuration. In addition, Yasari [40] successfully simulated V-shaped and oblique turbulent lean methane-air flames using the same approach on OpenFOAM. Furthermore, Ma *et al.* [15] studied the LES analysis of the ORACLES burner [41] using different algebraic source term equations from literature and gave a detailed error analysis of these equations.

The main idea behind the progress variable approach is to divide the domain into burned and unburned regions. The flame front is defined as the transition region from burned to unburned, using a scalar field. Therefore, continuity throughout the flame surface is an important factor in order to apply this method. Thus, laminar flamelet assumption should be valid in order to use the progress variable approach. In broken reaction zone, laminar flamelet assumption cannot be used. As a result, applicability of the progress variable approach is limited to laminar, wrinkled and corrugated flamelet regimes. Nonetheless, later closure rate modeling studies revealed that it can also be extended into thin reaction zones. In Figure 2.8, the experimental data used in this thesis for validation of the modified OpenFOAM code is plotted in a Borghi diagram [37]. Area inside the blue box represents the regions where laminar flamelet assumption can be made. For reference, in a Borghi diagram Otto engine is in corrugated flamelet region while gas turbines belong to thin reaction zone and Perfectly Stirred Reactor (PSR) burners are in broken reaction zone [42].

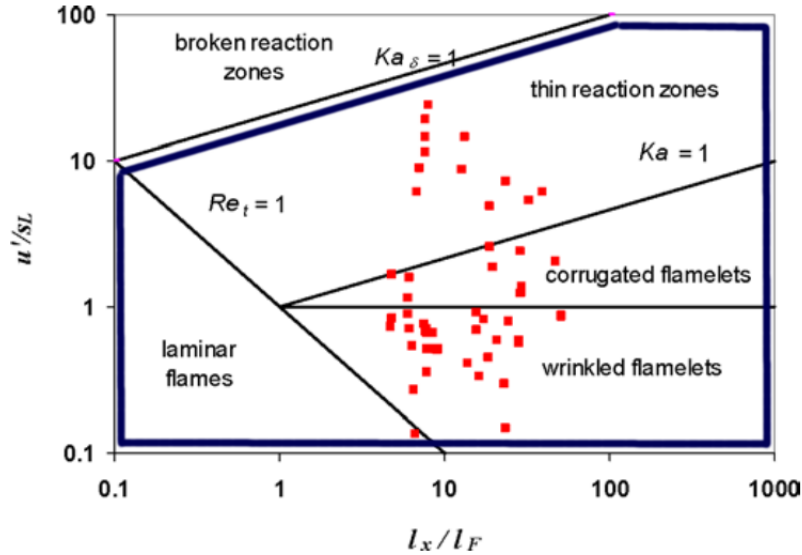


Figure 2.8: Flamelet regions of different experimental Bunsen flames used in the thesis. Area inside the blue frame represents the regions where laminar flamelet assumption is valid. [37].

2.4.5 Advantages of Progress Variable Approach

Although different simulation methods have been used intensively in different studies, each has its own advantages and disadvantages. While detailed chemistry approach gives the most detail on chemistry aspect of combustion, it requires really small grid spacing to capture the reaction zone within the flame and solving the chemistry in detail for each time step is computationally not feasible yet. In addition, while FGM method gives reasonably accepted results on the chemistry aspect of the combustion process, it is much more efficient since the chemistry is tabulated in a look-up table instead of solved every time step. However, pre-processing the look-up tables before the simulation is a tedious work and should be repeated if the thermophysical conditions change. Therefore, performing parameter sweeps in simulation is not feasible using FGM method, since each case would require its own unique look-up table.

As mentioned before, progress variable approach reduces chemistry and turbulence effects to the flame into a single transport equation and a source term to be modeled algebraically. Although progress variable approach does not provide in-depth information about the chemical aspect of the process, relatively good information on the

state of the process such as density, pressure and temperature fields and location of the flame front can be obtained. Solving a single transport equation allows running multiple cases with different thermophysical initial conditions in much short amount of time compared to other methods. Since parameter sweeps is the key aspect on improving existing combustor systems to meet the new emission criteria, a tool that quickly gives basic information on the system is needed a lot. After validating that the progress variable approach can be used in premixed combustion analysis with an acceptable error margin, the application area can be extended into full scale engine combustion in future.

CHAPTER 3

METHODOLOGY

In this chapter, Section 3.1 presents governing flow equations and turbulence models used in the simulations. Section 3.2 introduces the progress variable approach for premixed combustion modeling as well as explains governing equations and modeling techniques of this approach. Section 3.3 gives information on laminar flame speed and modeling approach used when calculating the laminar flame speed. Finally, Section 3.4 and 3.5 describe selected problem configurations, computational domain, boundary conditions and numerical schemes.

3.1 Governing Flow Equations

When solving fluid flow problems, governing conservation laws apply to fluid flow as to any other mechanical system. In most cases, Partial Differential Equations (PDE) for conservation of mass, momentum and energy need to be solved in order to simulate the viscous flow. The most common approach for solving these equations is the finite volume method, which discretizes the domain into small control volumes. This method solves governing equations in integral form for each and every control volume [43]. This thesis conducts premixed combustion simulations of different physical phenomenon using progress variable method within OpenFOAM framework. OpenFOAM is a C++ based open source library for CFD applications [44]. All the custom modifications are added to the OpenFOAM framework. In addition to OpenFOAM, Cantera is used to calculate thermodynamic aspects of simulations. Cantera is a suite of object-oriented software tools for problems involving chemical kinetics, thermodynamics, and transport processes [45]. It provides thermophysical results for 0D

and 1D flame configurations, which is useful in determining the initial and boundary conditions for the CFD simulations.

In this section, conservation equations solved for simulating fluid flow are introduced [46]. Additionally, brief information on sub-grid scale turbulence modeling is given.

3.1.1 Conservation of Mass and Momentum

Conservation of mass, also known as "continuity equation", states that time rate of change of mass in a control volume equals to the mass flow passing through its boundaries. Conservation of mass can be expressed as:

$$\frac{\partial \rho}{\partial t} + \nabla \cdot (\rho \vec{V}) = 0 \quad (3.1)$$

where \vec{V} is the velocity vector with x, y and z components. Regardless of the assumptions imposed on the flow behavior, conservation of mass is a necessary equation for all flow simulations and should be solved.

The conservation of linear momentum equation states that the time rate for the linear momentum change of a system equals to the sum of external forces acting on the system. It ensures that the system follows the Newton's second law. Linear momentum equation is formulated as:

$$\frac{\partial \rho u_i}{\partial t} + \nabla \cdot (\rho u_i \vec{V}) = 0 \quad (3.2)$$

It should be noted that this form of momentum equation does not contain any pressure effect. Pressure has to be computed separately and coupled with momentum equations. OpenFOAM solvers solve pressure separately and couples it to momentum equations.

Linear momentum equation is sufficient when solving for inviscid flows. However, almost all real fluid flow applications are viscous. Viscous behavior results in shearing and other stress effects, which should be taken into account by viscous effects into

the fluid motion formulation. When viscous stresses are included in the equation of motion by making simplifications using continuity equation, Navier-Stokes equations for compressible flows are obtained as [47]:

$$\begin{aligned}
\frac{\partial \rho}{\partial t} + \frac{\partial}{\partial x_i}(\rho u_i) &= 0 \\
\frac{\partial}{\partial t}(\rho u_j) + \frac{\partial}{\partial x_i}(\rho u_i u_j - \sigma_{ij}) &= 0 \\
\frac{\partial E}{\partial t} + \frac{\partial}{\partial x_i}(u_i E - u_j \sigma_{ij} + q_i) &= 0
\end{aligned} \tag{3.3}$$

where σ_{ij} is the stress tensor, \mathbf{E} is the energy density and q_i is the heat flux. While the first equation expresses conservation of mass, second governs conservation of momentum and the final deals with the conservation of energy. Navier-Stokes equations are enough to govern laminar, viscous flows. However, as the flow becomes turbulent, turbulent scales should also be resolved. Two different turbulence modeling approaches have been utilized in this thesis. The first one involves the modification of Navier-Stokes equations to calculate the mean and fluctuating velocity components by using Reynolds decomposition method. This method divides the velocity into mean and fluctuating components. Final form of the equations are known as Reynolds Averaged Navier-Stokes (RANS) equations, where extra stress terms arise because of the turbulent fluctuations. RANS is a robust approach used in turbulence modeling and widely popular in the academia and industry. However, the turbulence effect is presented in a time averaged form, hence accurately obtaining the instantaneous profiles is problematic.

Kolmogorov's theory explains that the large turbulent scales of the flow can be resolved and they depend on the geometry of the problem. However, smaller scales are independent from the geometry and considered as universal. The other approach, known as Large Eddy Simulation (LES) can solve large eddies using Navier-Stokes equations and models smaller scales through a sub-grid scale (SGS) model.

Using a filtering kernel, velocity can be represented with mean and fluctuating parts as:

$$u_i(x) = \int G(x - \xi) u(\xi) d\xi \quad (3.4)$$

$$u_i = \bar{u}_i + u'_i$$

After this, decomposed velocity (and pressure) is inserted to the set of equations in Equation 3.3. By filtering Equation 3.3, equation for the resolved field is obtained as:

$$\frac{\partial u_i}{\partial t} + u_j \frac{\partial u_i}{\partial x_j} = -\frac{1}{\rho} \frac{\partial p}{\partial x_i} + \nu \left(\frac{\partial^2 u_i}{\partial x_j^2} \right) + \frac{1}{\rho} \frac{\partial \tau_{ij}}{\partial x_j} \quad (3.5)$$

where the term $\frac{\partial \tau_{ij}}{\partial x_j}$ comes from non-linear advection, or turbulence.

While modeling this term, sub-grid scale turbulence models define the stress tensor with the SGS stress:

$$\tau_{ij} - \frac{1}{3} \tau_{kk} \delta_{ij} = -2\mu_t \bar{S}_{ij} \quad (3.6)$$

where \bar{S}_{ij} is the strain rate tensor and defined as:

$$\bar{S}_{ij} = \frac{1}{2} \left(\frac{\partial u_i}{\partial x_j} + \frac{\partial u_j}{\partial x_i} \right) \quad (3.7)$$

After this point, calculating the sub-grid scale viscosity ν_t varies. In this thesis k - ε RANS model and one-equation LES model are used, therefore k and ε needs to be calculated from strain rate tensor [48] as:

$$k_{sgs} = (C_s \Delta_s) |S|^2 / C_\mu^{1/2} \quad (3.8)$$

$$\varepsilon_{sgs} = (C_s \Delta_s) |S|^3$$

where Δ_s is filtering length and C_s, C_μ are model constants. Procedure in calculating sub-grid scale parameters differs from this point. The RANS turbulence modeling approach assumes local equilibrium while calculating the k_{sgs} . In addition, eddy viscosity ν_t can be defined through k and ε . If RANS is used, u' and eddy viscosity

v_t can be calculated using the relations in Equation 3.9. Whereas one equation eddy model, which is used in LES simulations, assumes that the k_{sgs} is not stationary and solves a transport equation, as presented in Equation 3.10 [49]. The eddy viscosity is then calculated using the relation given in the equation. After v_t is calculated, it is substituted back into the equation in order to obtain the final form, given in Equation 3.11.

$$\begin{aligned} u' &= \sqrt{\frac{2}{3}k_{sgs}} \\ l_x &= c_\mu^{3/4} \frac{(k_{sgs})^{3/2}}{\epsilon} \\ v_t &= c_\mu \frac{(k_{sgs})^2}{\epsilon} \end{aligned} \quad (3.9)$$

$$\begin{aligned} \frac{\partial(\rho k_{sgs})}{\partial t} + \frac{\partial(\rho \bar{u}_j k_{sgs})}{\partial x_j} - \frac{\partial}{\partial x_j} [\rho(v + v_t) \frac{\partial k_{sgs}}{\partial x_j}] &= \rho P_{k_{sgs}} - C_\epsilon \frac{\rho (k_{sgs})^{3/2}}{\Delta_s} \\ P_{k_{sgs}} &= 2v_{sgs} S_{ij} S_{ij} \\ v_t &= C_k (k_{sgs})^{1/2} \Delta_s \\ \Delta_s &= V^{1/3} \end{aligned} \quad (3.10)$$

$$\frac{\partial u_i}{\partial t} + u_j \frac{\partial u_i}{\partial x_j} = -\frac{1}{\rho} \frac{\partial p}{\partial x_i} + (v + v_t) \left(\frac{\partial^2 u_i}{\partial x_j^2} \right) \quad (3.11)$$

3.1.2 Energy Equation

The first law of thermodynamics states that the time rate for the increase of the total stored energy within the system equals to summation of the net time rate of energy addition by the heat transfer and the work into the system.

The set of equations required for solving compressible, viscous fluid flow can be satisfied by the energy equation coupled with mass and momentum equations. These equations should be also linked via ideal gas law:

$$p = \rho RT \quad (3.12)$$

3.2 Progress Variable Approach

In premixed combustion fuel and oxidizer are mixed prior to burning, therefore it is possible to represent the "burning state" by using a single scalar. As briefly introduced in the previous chapter, the main idea behind the progress variable approach is to model fully premixed combustion more inexpensively by dividing the domain into burned and unburned regions, as seen in Figure 3.1. Afterwards, species and energy equations replaced with a single scalar transport equation governing the flame motion, wrinkling and propagation.

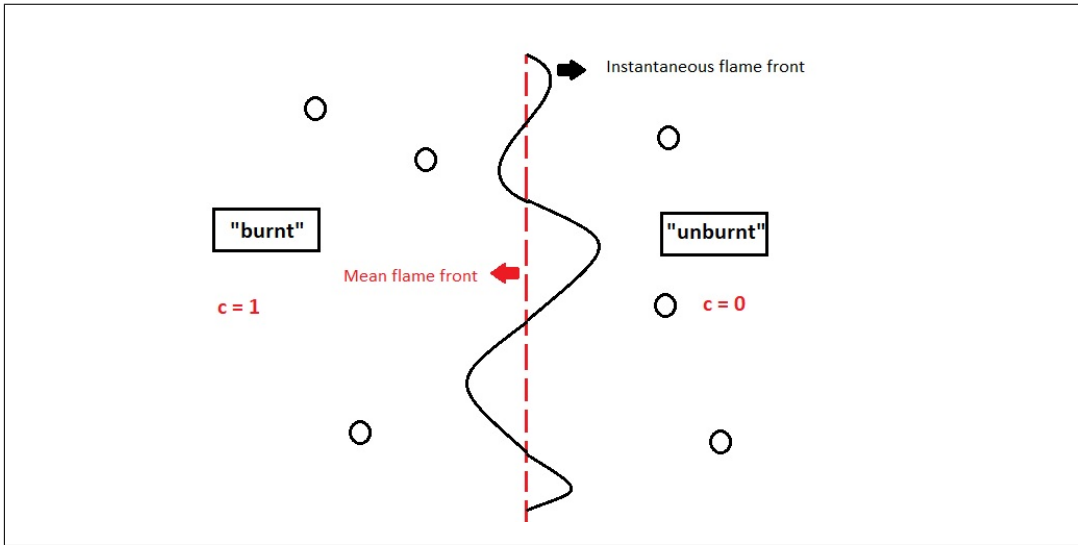


Figure 3.1: Schematic representation of progress variable approach

As presented in Equation 2.5, a progress variable "c" is introduced to represent the normalized temperature or the fuel mass fraction and the problem domain is divided such that the progress variable has the value "1" when the mixture is burnt and "0" when the mixture is unburnt. After defining a scalar to represent the flame front, a transport equation is obtained to replace species and energy equation as [16]:

$$\frac{\partial \bar{\rho} \tilde{c}}{\partial t} + \nabla \cdot (\bar{\rho} \tilde{u} \tilde{c}) = \nabla \cdot (\bar{\rho} \tilde{u} \tilde{c} - \overline{\rho u c} + \overline{\rho D_T \nabla \tilde{c}}) + \bar{w}_c \quad (3.13)$$

where D_T is the thermal diffusivity and \bar{w}_c is source term which should be modeled to include both the chemical and turbulence effects. Progress variable can be redefined

as "regress variable" by simply switching the definition of it in the burnt and unburnt regions. Although nothing changes in the formulation numerically, it is important to present the conversion, since the OpenFOAM solver for simulations uses regress variable approach [50]:

$$b = 1 - c \quad (3.14)$$

$$\frac{\partial(\rho b)}{\partial t} + \nabla \cdot (\rho \vec{u} b) - \nabla \cdot \left(\frac{\mu_t}{Sc_t} \nabla b \right) = w_c \quad (3.15)$$

where the diffusion coefficient D_T is replaced with the dynamic viscosity over Schmidt number, defining the ratio of momentum and mass diffusivity. One should note that by using the definition in Equation 3.14, the approach becomes *regress variable* approach. However, for the sake of consistency within this thesis, the term was kept as *progress variable* approach.

Different algebraic relations are proposed for modeling the source term w_c , which governs the chemical and physical effects on the flame propagation. The source term relation initially defined by Bray and Libby [51] as:

$$w_c = \rho_u S_u I_0 \Sigma \quad (3.16)$$

where S_u , I_0 and Σ are laminar burning velocity, stretch factor of the flame and flame surface density term respectively. Same study defines Σ term as:

$$\Sigma = \frac{c(1-c)}{L_y} \quad (3.17)$$

where L_y is the crossing length scale (thickness) of the flame. This formulation in the modeling approach ensures that the source term is only defined in the vicinity of the flame.

Some of the most recent approaches [15, 16, 37] involve combining Σ and I_0 term together to simplify modeling even further:

$$w_c = \rho_u S_u \Xi |\nabla b| \quad (3.18)$$

where S_u is the laminar flame speed and Ξ is the ratio of turbulent flame speed to the laminar flame speed, S_t/S_u . In this approach, $|\nabla b|$ term ensures that source term defined only at the vicinity of the flame front similar to Equation 3.17. In addition, Ξ term governs the effect of flow and chemistry to the flame and the laminar flame speed. The main task in turbulent premixed combustion simulations using progress variable approach is to model Ξ term accurately. Although reducing the effect of complex physical and chemical processes to a single transport equation accelerates the analysis process, modeling these effects with a single source term is not an easy task. Variety of different algebraic models have been developed ranging from simple algebraic closure relations [52, 53] to complex ones developed from fit functions for experimental results. Ma *et al.* compared the performances of different algebraic closure equations and investigated their performance [15]. An algebraic formulation derived from the experimental data for turbulent premixed Bunsen flames gave the best results among them. Derived by Muppala *et al.* [37], this relation is given as:

$$\Xi = \frac{A_T}{A} = 1 + \frac{0.46}{Le} Re_t^{0.25} \left(\frac{u'}{S_u}\right)^{0.3} \left(\frac{p}{p_0}\right)^{0.2} \quad (3.19)$$

where Le , Re_t , u' and p_0 are Lewis number (ratio of thermal diffusivity to mass diffusivity), turbulent Reynolds number $Re_t = \frac{u' \ell_x}{\nu}$ (ℓ_x integral length scale and ν kinematic viscosity), turbulent velocity fluctuations and reference pressure of 0.1 MPa, respectively. The u' and ℓ_x terms are calculated using the relations introduced in Equation 3.9.

By default, OpenFOAM solver used in simulations utilizes the algebraic relation introduced in [54]:

$$\begin{aligned} \Xi_{eq}^* &= 1 + 0.62 \sqrt{\frac{u'}{S_u}} Re_t \\ \Xi_{eq} &= 1 + 2(1 - b)(\Xi_{eq}^* - 1) \end{aligned} \quad (3.20)$$

Although Equation 3.20 is successful for capturing the flame behavior in quasi steady cases such as Bunsen burners, simulation of the flame wrinkling phenomena in more turbulent cases could not be achieved. Developer of the model stated that the flame

surface instability model is very sensitive to the case setup and numerical schemes used, thus making it difficult to get a reliable validation case [55]. Therefore, Equation 3.19 is used instead.

It should be noted that the progress variable approach makes a crude assumption of fully burned and unburned regions divided by a continuous flame front surface, similar to Figure 2.7. In Figure 2.8, where the Borghi diagram including the flamelet information of experimental Bunsen flames used in the study is presented, it can be seen that the application of the progress variable approach is only limited to the cases where flame front can be represented by continuous laminar flamelets. In this approach the chemistry inside the flame is only represented by a single step global reaction. Instead of resolving the chemical scales in detail, flow effects to the flame shape and wrinkling are modeled through Ξ term in Equation 3.18. By neglecting the chemistry inside the flame, it is highly unlikely to get realistic results for the chemical compositions within the reaction zone region. The main idea behind the progress variable approach is to give information on flame front position and the effect of flow to the flame shape and wrinkling. In order to achieve this, various modeling techniques are used for simulating the effect of combustion. Further comments on this approach and other alternative approaches will be discussed in Chapter 4 and 5.

3.3 Laminar Flame Speed

This thesis mainly focuses on the effect of flow and thermophysical characteristics to the turbulent burning velocity during the combustion process. Calculating the laminar flame speed closer to the actual value is important for obtaining accurate results. Although the experimental results for different reactants show that the laminar flame speed can be measured with a certain accuracy, there are still deviations from one experimental result to another. The same problem can be seen in the detailed chemistry approach. Different mechanisms used in simulating the flame yields close but still different laminar flame speed values, as illustrated in Figure 3.2 [56].

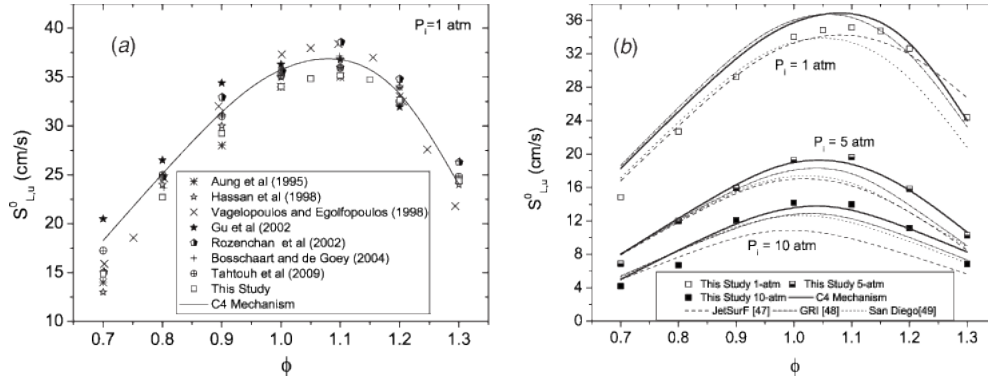


Figure 3.2: Results of different reduced mechanisms on n-dodecane combustion

Laminar burning velocity depends on composition of the mixture, pressure and unburnt temperature [1]. Gülder [57] derived a correlation to estimate the laminar flame speed of different propane, ethylene, methane and iso-octane mixtures using a fitting function on empirical data for certain pressure and temperature ranges. Although extended ranges still give accurate results to a certain point, initial work states that the correlation is valid for an unburned temperature up to 600 K and around 1 atm pressure. The full formulation of Gülder correlation is [50]:

$$S_u = W \phi^\eta \exp[-\xi(\phi - 1.075)^2] \left(\frac{T}{T_0}\right)^\alpha \left(\frac{P}{P_0}\right)^\beta \quad (3.21)$$

where ϕ is the equivalence ratio, T_0 and P_0 are reference parameters of 300 K and 1 atm, T is unburned temperature and η , ξ , α , β are equation constants for different reactants. Table 3.1 gives constants provided by OpenFOAM for a number of different reactants.

Table3.1: Gülder correlation constants for different reactants

Reactant Name	W	η	ξ	α	β
Methane	0.422	0.15	5.18	2	-0.5
Propane	0.446	0.12	4.95	1.77	-0.2
Iso Octane	0.4658	-0.326	4.48	1.56	-0.22

In order to re-validate the accuracy of Gülder’s correlation, a sweep for equivalence ratio in constant pressure and temperature conditions is performed using Cantera and

the obtained laminar flame speed results are compared with Gülder's correlation results:

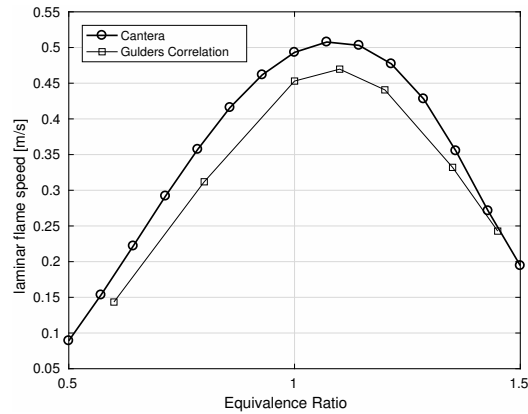


Figure 3.3: Laminar flame speed for methane flame at $T = 300$ K and $p = 1$ atm

The results for Gülder's correlation seems to be in an acceptable range. Therefore, it is used in the algorithm for calculating the laminar flame speed.

3.4 Problem Configurations

Three different cases are investigated to assess the performance of the progress variable approach on the OpenFOAM framework, which uses Equation 3.20 as the default reaction closure term. Before going any further, the source code is modified to use the rate closure equation given in Equation 3.19.

3.4.1 2D Bunsen Burner (RANS)

As a verification and validation case, 2D analysis of different Bunsen burner cases are carried out with RANS turbulence modeling to assess the performance of Equation 3.19. These results are then compared to the experimental data from [6], which Equation 3.19 is derived by using a fitting function on experimental data.

Investigated Bunsen flames have a burner exit with a diameter of 20 mm. To create a grid with boundaries far away from each other and not effecting the flame shape, 2D computational domain in the simulations is extended to 10 times the exit radius in the

radial direction and 15 times in the height. 2D structured grid with equidistant grid spacing is used with an approximate grid resolution of 2.5 grid/mm, thus leading to approximately 50,000 grid points in whole domain, as seen in Figure 3.4.

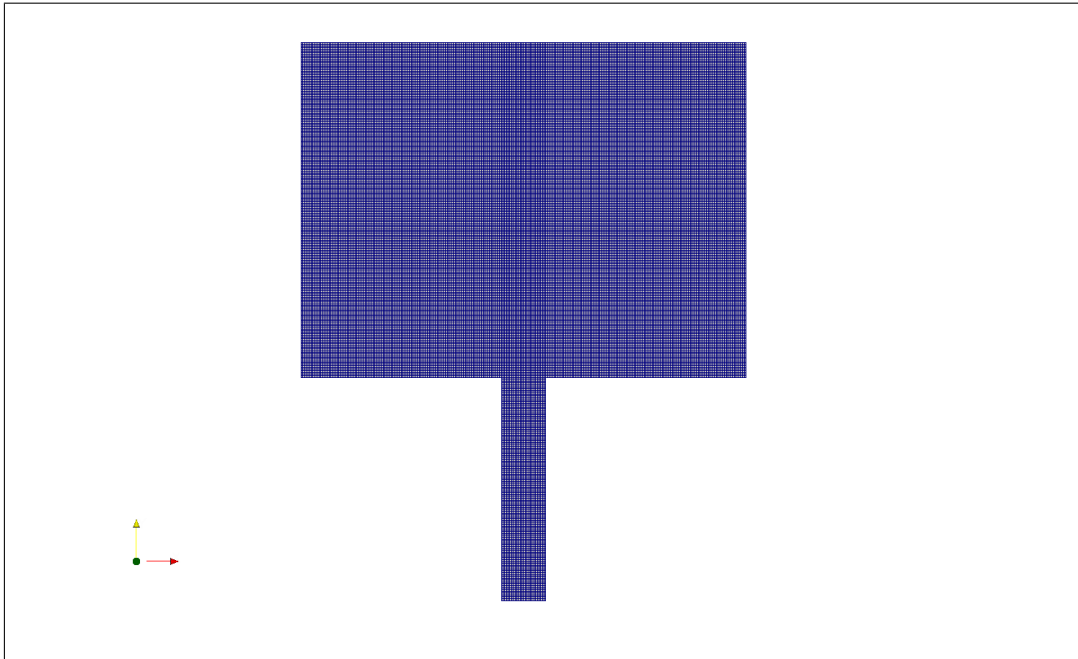


Figure 3.4: Computational domain for 2D Bunsen flame analysis

Simulation parameters such as ambient pressure, velocity fluctuation at the inlet, and the inlet velocity are taken from the experimental data in [37] and given as initial conditions to OpenFOAM. For turbulence modeling, k - ε turbulence model is used. Inlet values for k and ε are calculated from the given velocity fluctuation and integral length using Equation 3.9, where $c_\mu = 0.09$ and ℓ_x is the characteristic integral length from experimental results.

Thermophysical properties such as density, viscosity, specific heat and enthalpy are required to perform the combustion simulations. In order to determine these parameters, Cantera is used to simulate the free flame with the same initial conditions. After the values for reactants and products are determined, results are used as initial conditions for burned and unburned regions in the flow simulation. In Figure 3.5, 1D free flame analysis for propane with $\phi = 0.9$, $T_{initial} = 300$ K and $p = 0.5$ MPa is presented. Cantera cases can be run through Python scripts recursively, which makes it easy to

perform parameter sweeps when needed.

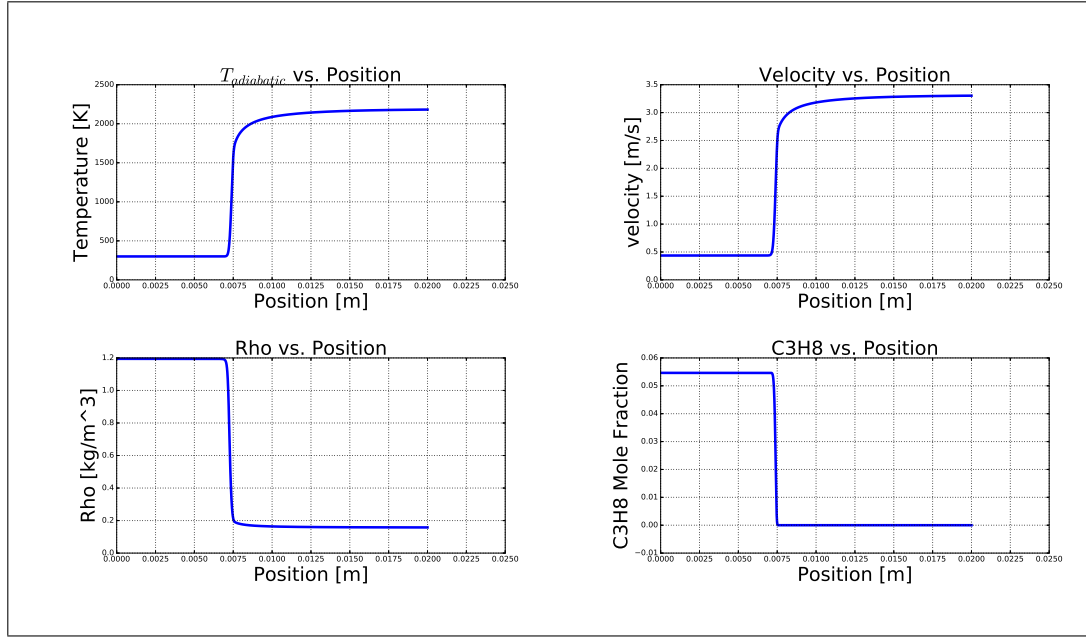


Figure 3.5: Cantera results for $\phi = 0.9$, $T_{initial} = 300$ K and $p = 0.5$ MPa

Before the effects of flow parameters on the closure reaction term is investigated, pressure and equivalence ratio sweeps are performed while keeping flow parameters constant to investigate the effect of thermophysical factors to Equation 3.19. After the validation of compatibility with different thermophysical conditions, 3 cases of propane combustion with $\phi = 0.9$ and $p = 0.5$ MPa are selected to investigate the effect of flow parameters on the closure rate equation. Details for these cases are given in Table 3.2.

Table3.2: Simulation parameters for $T = 300$ K

Fuel	ϕ	p (MPa)	u' (m/s)	ℓ_x (mm)	U (m/s)	ρ (kg/m ³)	$\nu \times 10^6$ (m ² /s)	S_u (m/s)	Experiment S_T/S_u
C ₃ H ₈	0.9	0.5	0.20	0.96	2.76	5.89	3.05	0.26	3.50
C ₃ H ₈	0.9	0.5	0.49	1.10	2.62	5.89	3.05	0.26	4.15
C ₃ H ₈	0.9	0.5	1.4	1.25	8.14	5.89	3.05	0.26	7.31

After the cold flow is simulated for approximately after 500 time steps, outlet boundary of the domain is set to $b = 0$ and the propagation of the progress variable from this initial condition is investigated. When the convergence is achieved, time averaging is performed on the progress variable field and the results are compared to the

experimental results in [37] and [6].

3.4.2 3D Bunsen Burner (LES)

After validating Equation 3.19 with a quasi-steady 2D case, the same problem configuration is extended to 3D domain to show that the same model can also be utilized for 3D LES simulations. 3D LES simulations are performed for Bunsen flames with different S_u/U ratios to show how flame behavior changes with different flame speeds. This case is also used to demonstrate the performance of the source term reaction equation for capturing flame wrinkling phenomena. In addition, further information on applicability limits of progress variable approach is obtained. Since LES turbulence modeling used, turbulence parameters like u' and eddy viscosity are obtained from Equation 3.10.

The computational grid consists of approximately 2 million cells. As represented in Figure 3.6, it mostly concentrates near inlet pipe and the mid plane to capture the Bunsen flame accurately. Same numerical and boundary conditions of 2D Bunsen flame simulations are utilized by only changing the turbulence modeling approach to one equation eddy LES method.

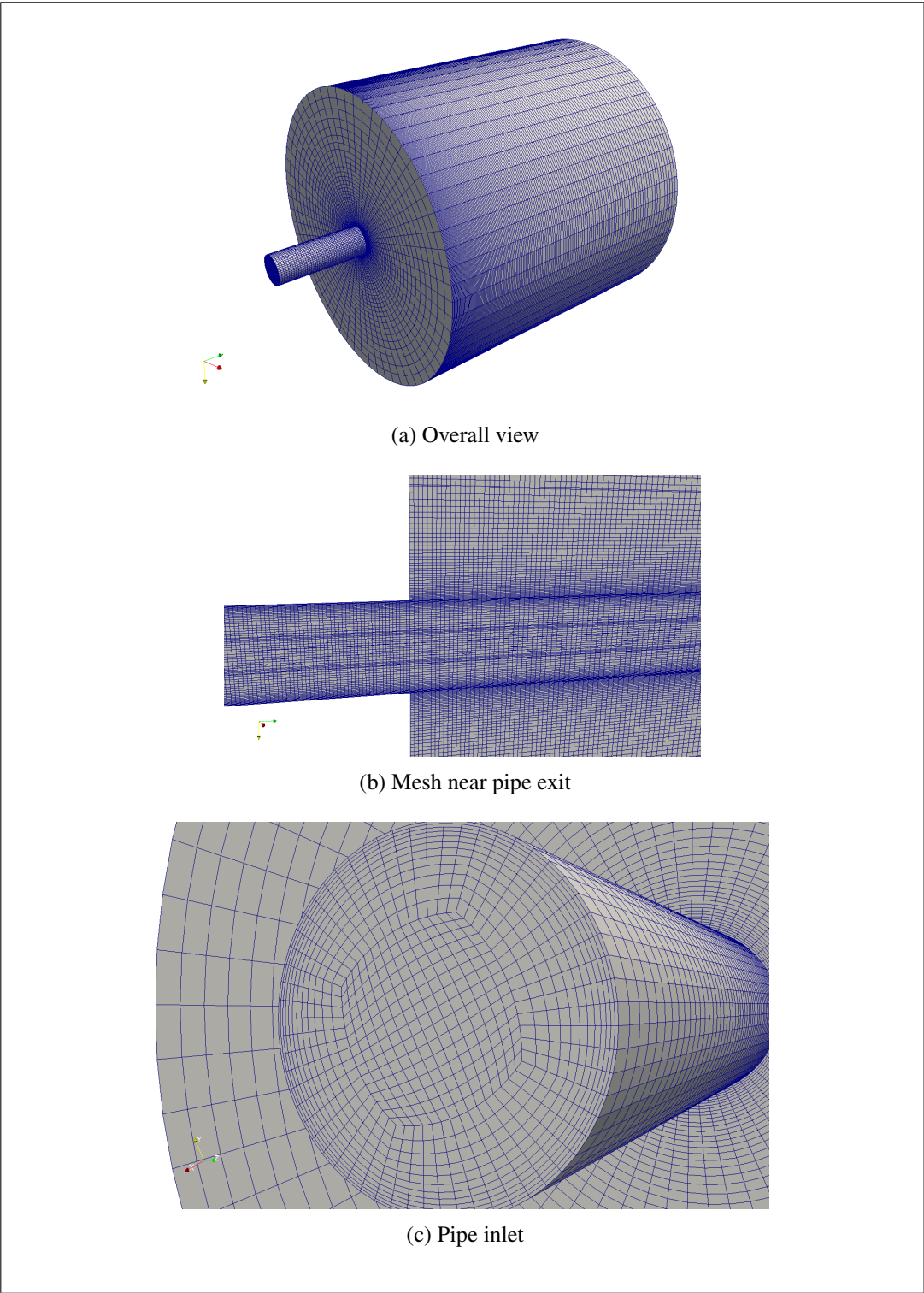


Figure 3.6: Computational domain for 3D bunsen burner

3.4.3 Backward Facing Step

After its applicability on LES simulations is validated, the same closure equation is then applied to the analysis of reacting backward facing step experiment [58]. Dimensions for the setup is given in Figure 3.7, where step height h is 0.0254 m. Equation 3.19 has been proved to be compatible with LES turbulence configurations as well as RANS simulations [38], which enables the usage of one-equation eddy LES turbulence model approach to model the sub-grid scale turbulence in the domain. Computational domain consists of approximately 1 million cells, as represented in Figure 3.8. Grid is refined near shear layer regions and walls to ensure that $y^+ < 1$ condition is satisfied. Cyclic boundary condition is used in the span-wise front and back walls to create infinitely long duct effect in z direction.

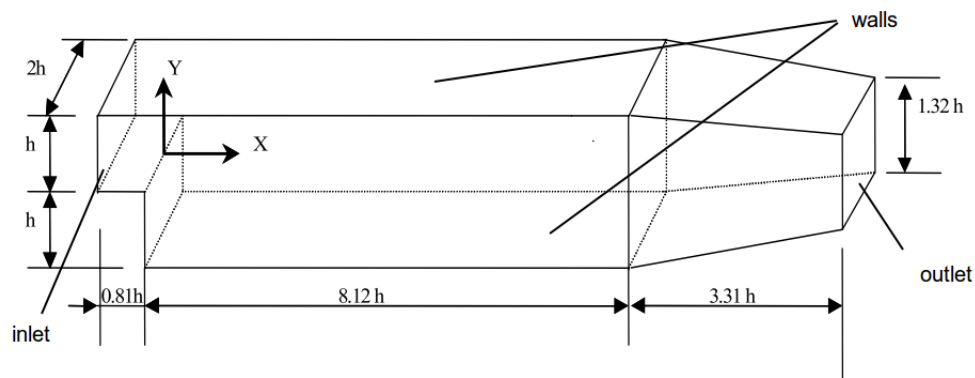
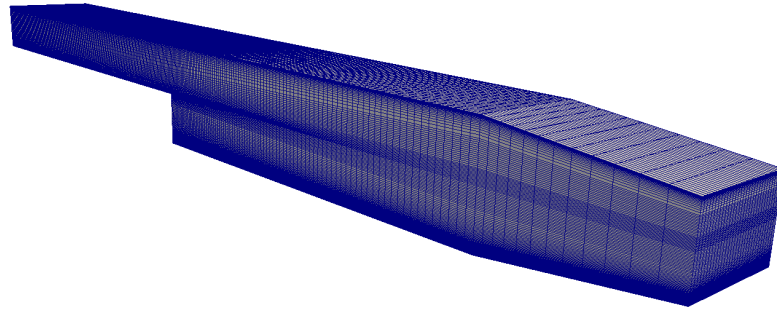
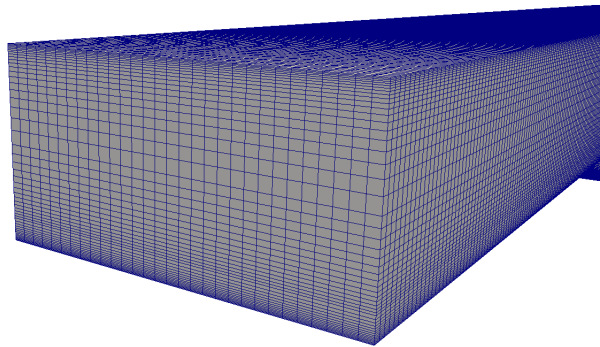


Figure 3.7: Schematic of the backward facing step problem domain [53]



(a) Overall view



(b) Channel inlet

Figure 3.8: Computational domain for backward facing step

The experimental data for Bunsen flames is available for a wide range of flow conditions and 3 different type of fuels: methane, ethylene and propane. However, data on the backward facing step case is only available for propane. Therefore, the simulations are limited to propane only.

Several studies have investigated numerical simulation of backward facing step experiment by making simplifications and assumptions such as utilizing wall functions, mimicking turbulence by introducing small perturbations at the inlet rather than using a developed profile [53, 59]. Criteria for assessing the performance of Equation 3.19 should be selected adequately due to the high Reynolds number of the problem

configuration and having available reacting flow data only for the mass fraction of CO_2 from the experiment. CO_2 is the final product of the combustion and its concentration highly depends on the chemical reactions inside the flame, which is not taken into account in the progress variable approach. To be able to investigate the performance of the model and the closure rate equation, non-reactive flow is simulated first. Time averaged mean and fluctuating velocity statistics are then compared with the experiments to validate the mesh, numerical models and solver configurations. After the case is validated, reacting flow is simulated and time averaged progress variable results are compared with CO_2 concentrations, and similar trends in the profiles are investigated. Flame wrinkling of the flame front surface is investigated in instantaneous profiles and compared to Schlieren images. Finally, re-circulation length of both non-reactive and reactive flow is compared to the experimental results.

3.5 Numerical Methods and Boundary Conditions

For all cases, the governing equations are discretized on collocated grid by using finite volume approach. Second order spatial and temporal discretization schemes are selected to ensure enhanced accuracy. In backward facing step case, to ensure numerical stability, cell-limited second order schemes are used for gradient terms. Central differencing scheme is selected for momentum equation, which ensures reduced numerical diffusion and increases accuracy. In backward facing step case, in order to create turbulent inlet flow conditions, a cross section along the inlet pipe is selected 150 mm downstream from the inlet and U and k fields are fed back to the inlet, creating an infinitely long channel to create turbulent effects easier. For each case different boundary conditions are used. In 2D and 3D bunsen burner cases, fixed inlet velocity is used with no-slip pipe walls. To prevent the pressure waves bouncing back into domain, wave transmissive boundary condition for pressure is used in outlet for all cases. To ignite the field a burned scalar region should be initialized so that flame can progress from that initialization. For all cases, one of the boundaries set the burned to initialize the flame. For bunsen burner cases the outlet, for backward step case the step wall was used for this purpose. Boundary conditions are presented in Table 3.3.

Table3.3: Boundary conditions

	2D Bunsen Burner	3D Bunsen Burner	3D Backward Step
U	Fixed Inlet No-Slip Walls Pressure Outlet	Fixed Inlet No-Slip Walls Pressure Outlet	Mapped Inlet No-Slip Walls Pressure Outlet
p	Wave Transmissive Outlet Zero gradient elsewhere	Wave Transmissive Outlet Zero gradient elsewhere	Wave Transmissive Outlet Zero Gradient elsewhere
k	Fixed Inlet Wall Function Walls Zero Gradient Outlet	Fixed Inlet Zero gradient elsewhere	Mapped Inlet Zero gradient elsewhere
ϵ	Fixed Inlet Wall Function Walls Zero Gradient Outlet	-	-
Regress variable	Fixed inlet ($b = 1$) Fixed Outlet ($b = 0$) Zero gradient elsewhere	Fixed inlet ($b = 1$) Fixed Outlet ($b = 0$) Zero gradient elsewhere	Fixed inlet ($b = 1$) Fixed Step Wall ($b = 0$) Zero gradient elsewhere
Other scalars	Zero Gradient / Calculated	Zero Gradient / Calculated	Zero Gradient / Calculated

CHAPTER 4

RESULTS

This chapter presents the results of the modified progress variable solver with Equation 3.19 in the OpenFOAM framework. After validating the closure equation in Section 4.1 with the experimental data from [6], 3D analysis of Bunsen flame is investigated in Section 4.2. 3D Bunsen burner simulation is conducted as a demonstration step to show the applicability of Equation 3.19 on LES simulations. As a final case, backward facing step for $Re = 22,000$ is investigated in Section 4.3.

4.1 2D Bunsen Burner

As a preliminary analysis, Bunsen flames are simulated by sweeping through pressure and equivalence ratio to observe the effect of change in thermophysical properties. For pressure sweep, equivalence ratio was taken as constant $\phi = 0.9$ and for equivalence ratio sweep pressure was taken as 0.1 MPa.

Pressure sweep presented in Figure 4.1 reveals that with increasing pressure, turbulent flame speed increases and Bunsen cone becomes smaller. Relations in Equation 3.19 and 3.21 clearly show that increasing pressure increases both laminar flame speed calculated from Gülder's correlation and the Ξ term, which results in increased turbulent flame speed.

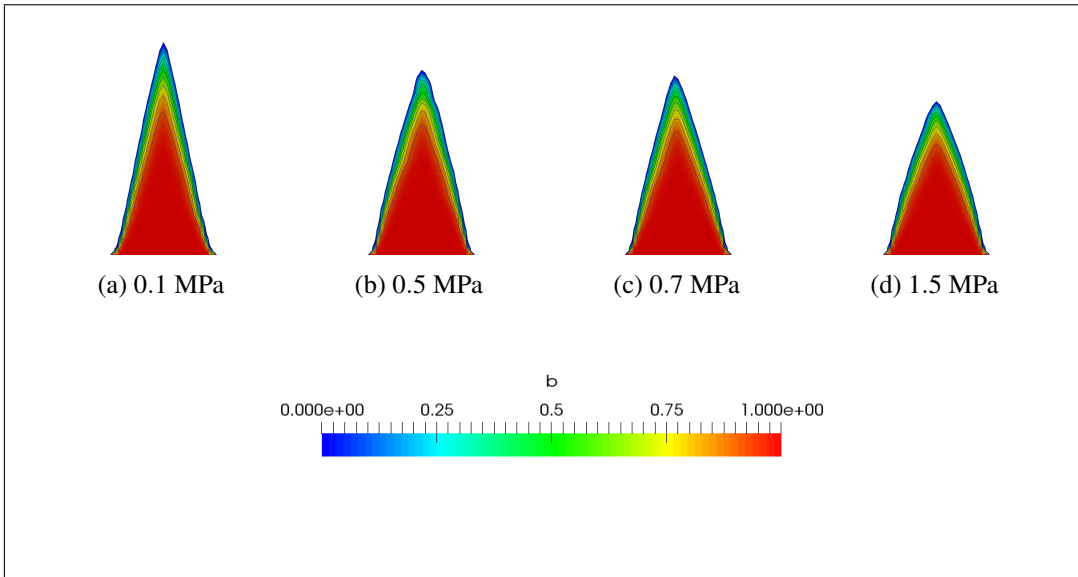


Figure 4.1: Time averaged progress variable flame shape for different pressure values

The most dominant thermodynamic property effecting the overall flame behavior is the equivalence ratio. Sweeping through different equivalence ratio values reveals that the turbulent flame speed is highly dependent to this parameter. Equivalence ratio highly affects the laminar flame speed, which also results in affecting the turbulent flame speed. It can be seen that flame shapes in Figure 4.2 are correlated with the changing trend of the laminar flame speed with respect to the equivalence ratio, as presented in Figure 3.3. Furthermore, Cantera simulations revealed that with increasing equivalence ratio, kinematic viscosity decreases, which results in an increase in Reynolds number. Increase in the Reynolds number also increases Ξ and turbulent flame speed. However, this effect is much smaller compared to the effect of laminar flame speed.

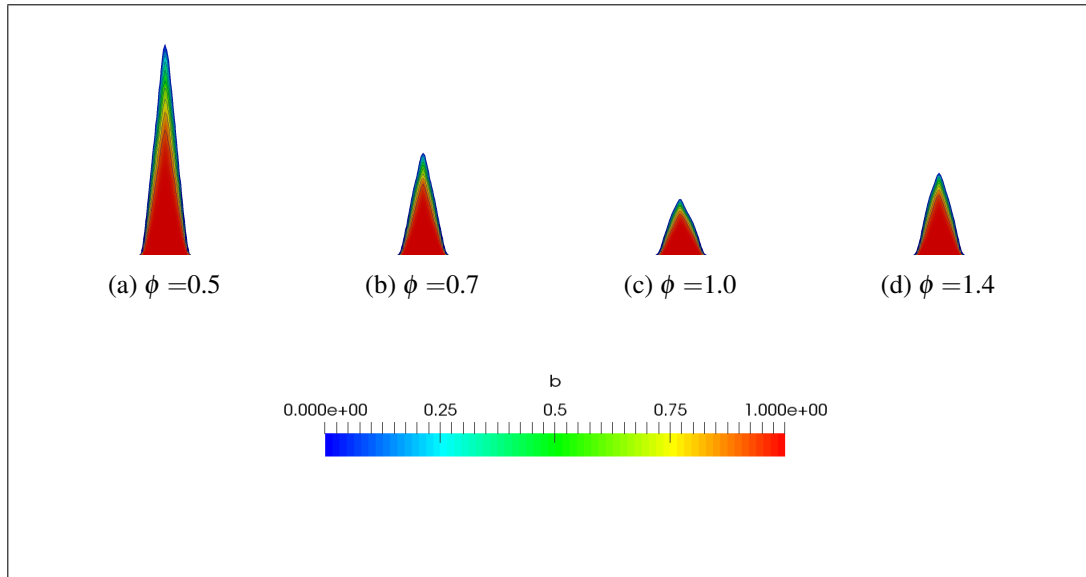


Figure 4.2: Time averaged progress variable flame shape for different equivalence ratio values

By using progress variable approach and constant enthalpy assumption in the burned and unburned regions, all thermodynamic parameters are coupled with a scalar b , which represents burned as 0 and unburned as 1. Examples of this coupling can be seen later in Figure 4.16, where instantaneous progress variable, density and temperature fields for backward facing step are presented. For each specific case, free flame simulations are conducted with Cantera to determine the enthalpy, viscosity and adiabatic temperature of the flame. These flame conditions are used as initial conditions in the simulation. Figure 4.3 shows the variation of the temperature and density across the flame. The data is plotted from centerline of the nozzle outlet in the axial flow direction. These profiles clearly show that the density is higher in the unburned region and decreases across the flame. In addition, the unburned density value is around 5.9 kg/m^3 , which is consistent with the experimental values in Table 3.2 for same pressure and ϕ configuration.

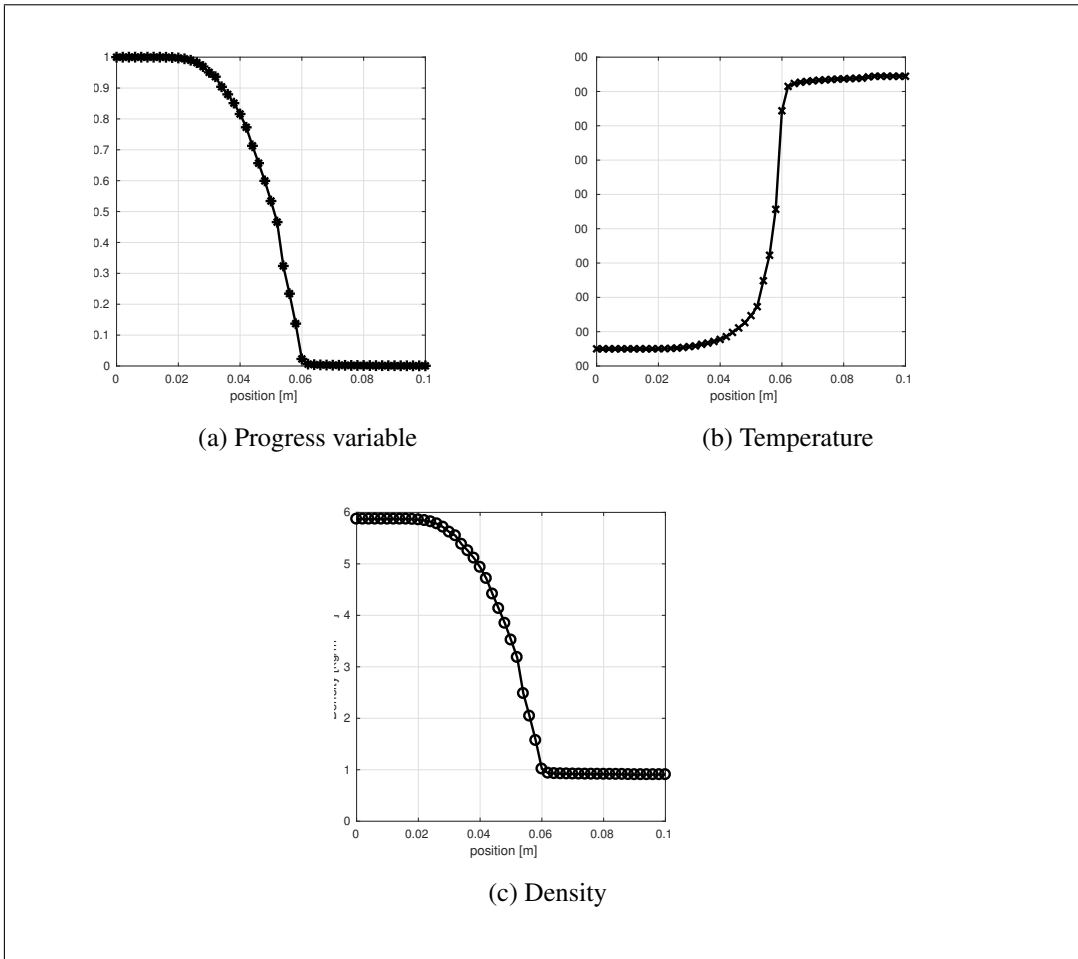


Figure 4.3: Change of thermodynamic values across the flame for $\phi = 0.9$ and $p = 0.5$ MPa

After performing the thermophysical sweep simulations and ensuring that the rate closure equation behaves physically as expected, comparison with the experimental results are made to assess the accuracy of the model. Although Muppala *et al.* [37] utilized the same closure rate equation and compared the findings with experimental data, it is important to investigate the fidelity of the implementation of closure rate equation and its compatibility with the OpenFOAM framework.

Since the effect of change in pressure and equivalence ratio is investigated and their behavior is validated, test cases are selected with the constant pressure and the equivalence ratio with other varying flow conditions, such as velocity fluctuations and the inlet velocity. Therefore, three propane flame cases presented in Table 3.2 are used to

validate the closure rate equation in OpenFOAM. Resulting progress variable fields are presented in Figure 4.4. It can be seen that the flame profiles obtained by time averaged progress variable fields are visually consistent with the averaged experiment results.

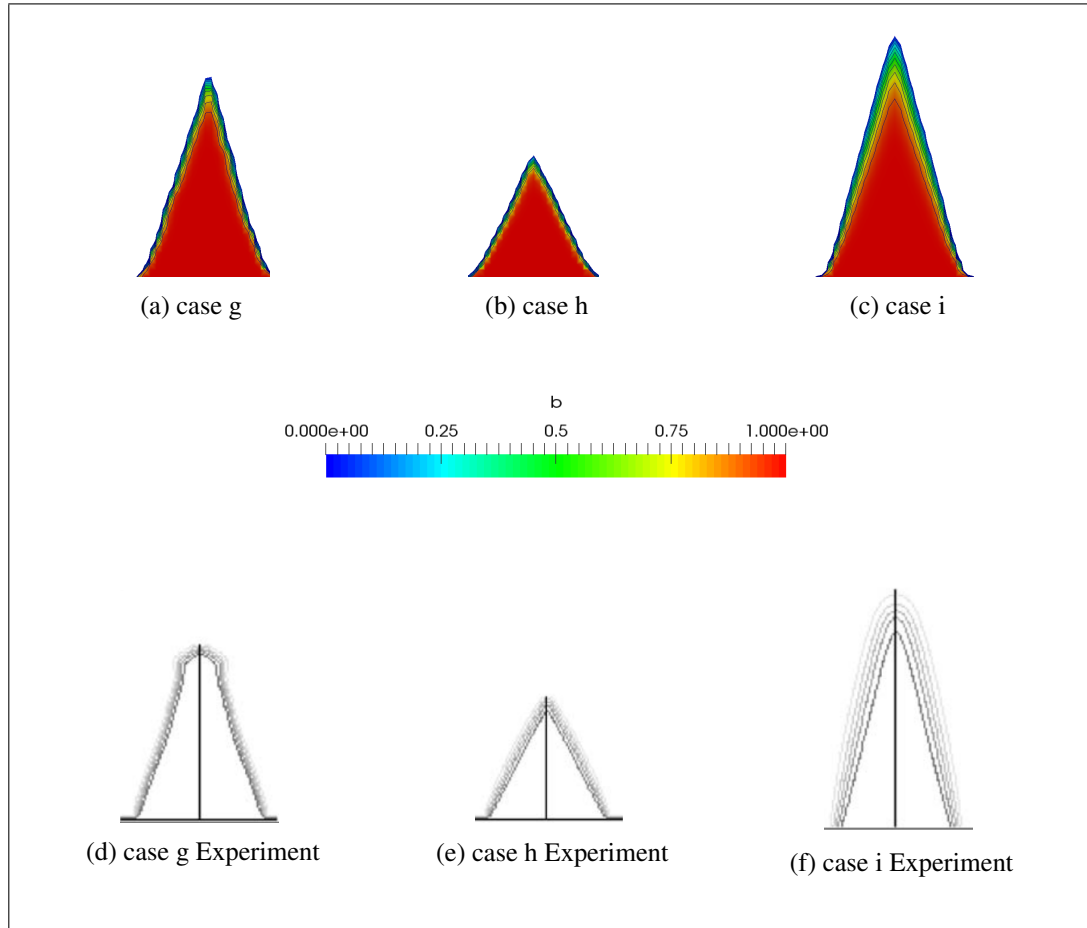


Figure 4.4: Calculated Bunsen flame profiles with time averaged progress variable

One other parameter that should be investigated is the non-dimensional flame angle, represented by S_t/S_u . In Figure 4.5, a basic schematic for the flame speed - inlet velocity balance is presented. This figure states that the turbulent flame speed that is normal to the oblique flame front should be in balance with the inlet velocity. If the half angle of the flame is denoted as θ , relation can be written as:

$$S_t = U \sin(\theta) \quad (4.1)$$

The results show that Equation 3.19 is successful in estimating the turbulent flame speed for propane flames. In addition, Bunsen flame profiles presented in Figure 4.4 show that flame front position and flame shapes are calculated correctly. The continuous lines seen at the flame front region in Figure 4.4 represent the progress variable iso-contours from $b = 1$ to $b = 0.9$. Therefore, presented flame shapes illustrate the unburned flame region of the Bunsen flame and disregard the transition region of the flame since chemical scales are not resolved in that region. Since the performance of the rate closure equation is validated for propane flames, the analysis can be extended to 3D domain.

4.2 3D Bunsen Burner

After validating Equation 3.19 with 2D Bunsen flame cases, the analysis is extended to 3D to verify the applicability of the method in 3D simulations. To demonstrate the performance of the model in capturing flame wrinkling phenomena, three points are chosen in Borghi Diagram to represent three different turbulent flame regimes, as seen in Figure 4.6. Due to the limited resources, the simulations were carried out for only these three cases.

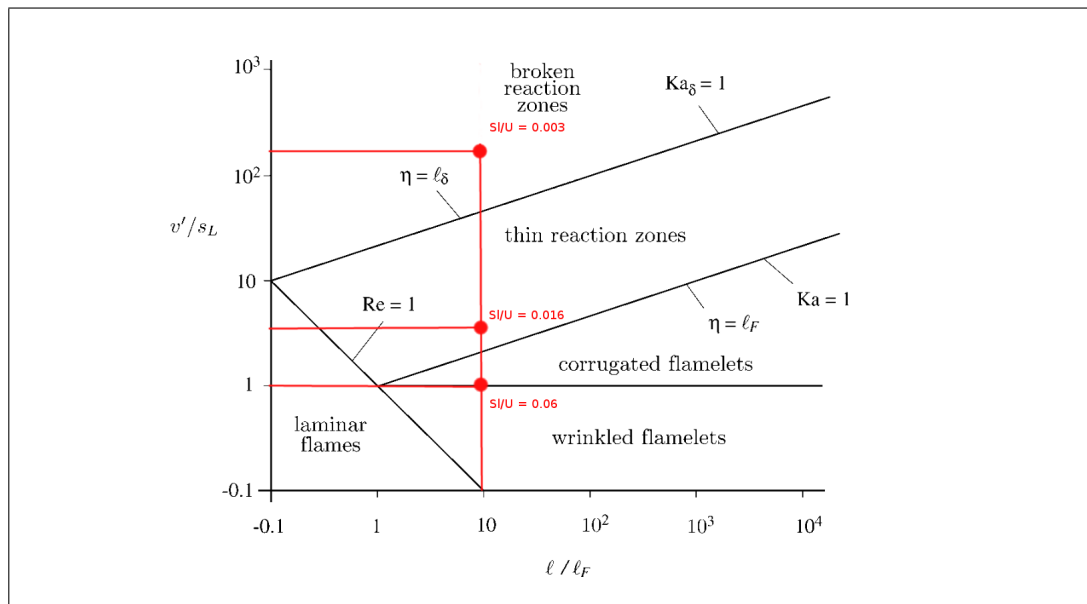


Figure 4.6: 3D bunsen flames on Borghi diagram

Using the S_u/U values in these points with same thermophysical properties, 3 different cases are simulated and compared. One equation eddy LES turbulence model is used with the constant turbulence kinetic energy at the inlet. Similar to 2D Bunsen burner analysis, thermophysical parameters are given as initial conditions from the Cantera simulation. Resulting fields are represented by cutplanes in Figure 4.7. In spray flame analysis, Wehrfritz *et al.* [30] reported that the fuel-rich core region of the spray would have premixed combustion characteristics. In Figure 4.7a, it can be seen that the domain clearly has distinct burned and unburned regions near the core of the flame, which later diffuse into each other at downstream regions. Also, it can be seen that in low laminar flame speed configuration, the progress variable approach successfully captures the flame *blow off* phenomena. Furthermore, wrinkling of the flame interface affected from the velocity fluctuations can be clearly observed for the first phase of the flame, which is located at the first 5 to 6 diameters length from the nozzle exit in the streamwise direction.

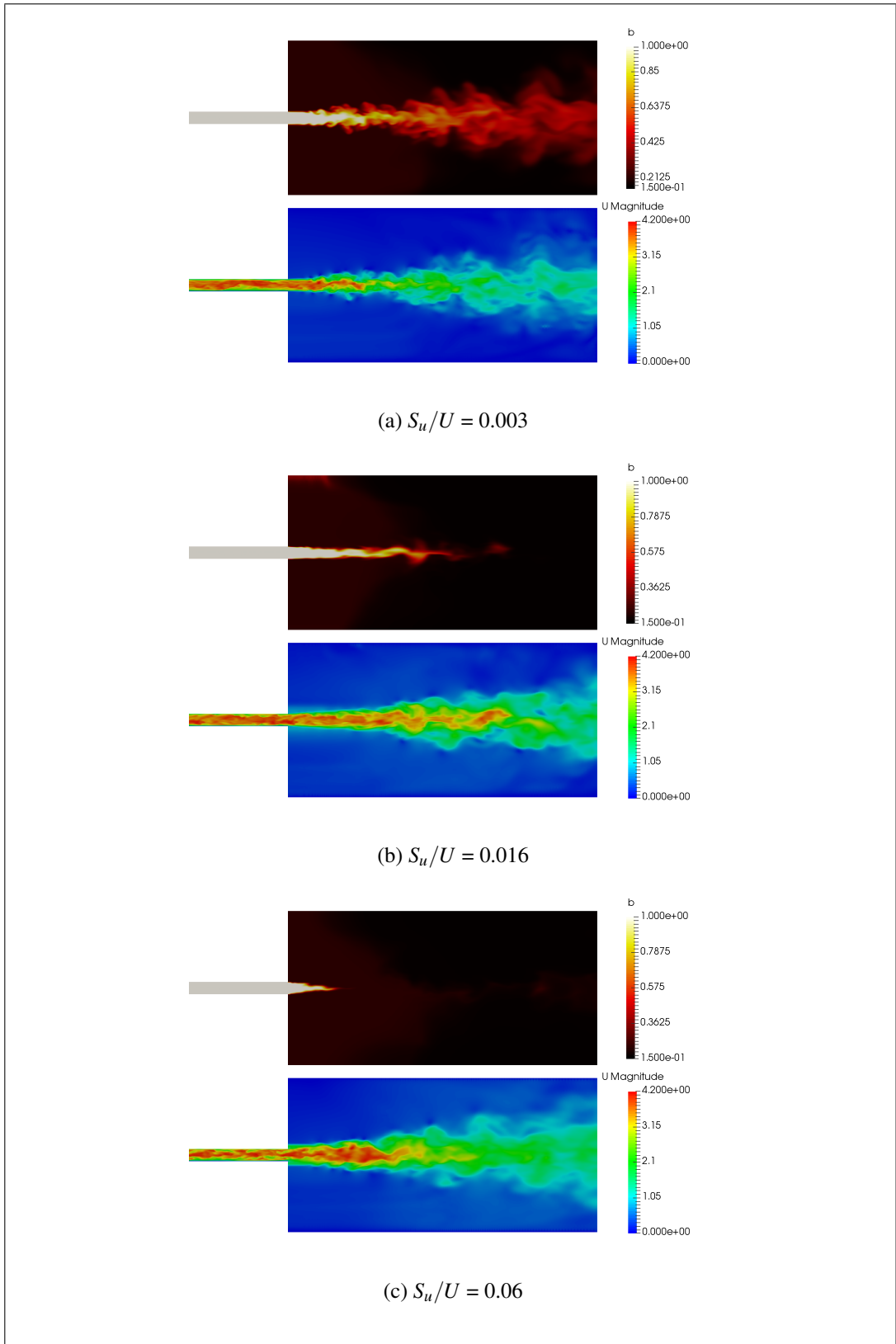


Figure 4.7: Instantaneous progress variable and velocity magnitude profiles for different S_u/U configurations

If Borghi diagram presented in Figure 2.5 is examined, it can be seen that by increasing the laminar flame speed, the configuration tends to become less corrugated, since u'/S_L value is decreasing. Thus, if laminar flame speed is increased, the flame front would become less wrinkled. Figure 4.7b is obtained by increasing the laminar flame speed while keeping the inlet velocity constant, thus S_u/U ratio. It can be clearly seen that the wrinkled profiles around the flame front became flatter. This is due to the fact that increased burning speed dominates over the wrinkles caused by the turbulent eddies in the domain. The burned region has lower density and higher kinematic viscosity than the unburned, which causes the turbulent behavior to die out. With reduced turbulent effects, flame becomes flatter. Schematic representation of flame wrinkling is given in Figure 4.8. κ represents the curvature effect, which dominates over unstretched laminar burning velocity with increasing turbulent effect. As the turbulent intensity increases, flame will wrinkle more and finally corrugate. Further at some point the continuous laminar flamelet will be broken, which would result with broken reaction zone, where progress variable approach is not valid.

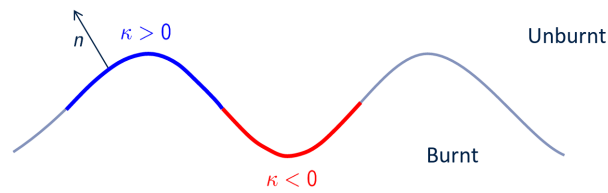


Figure 4.8: Schematic representation of flame wrinkling [60]

Finally, if laminar burning speed is increased even more, Figure 4.7c is obtained. The Bunsen cone formed by the flame front is clearly visible. The S_u value is so high that this configuration corresponds to the laminar-wrinkled flamelet regime in the Borghi diagram.

Karlovitz number, which is defined and introduced in Equation 2.1, can be used to assess the flamelet regime of each case. Simplifying the relation, Karlovitz number can be represented as the ratio of the turbulence intensity to flame speed, which corresponds to the y axis value of the Borghi diagram. The ratio of turbulent length scale to flame thickness can be taken to be in the order of 10 for simplification. In addition, cutplanes with time averaged Karlovitz number values are presented in Figure 4.9.

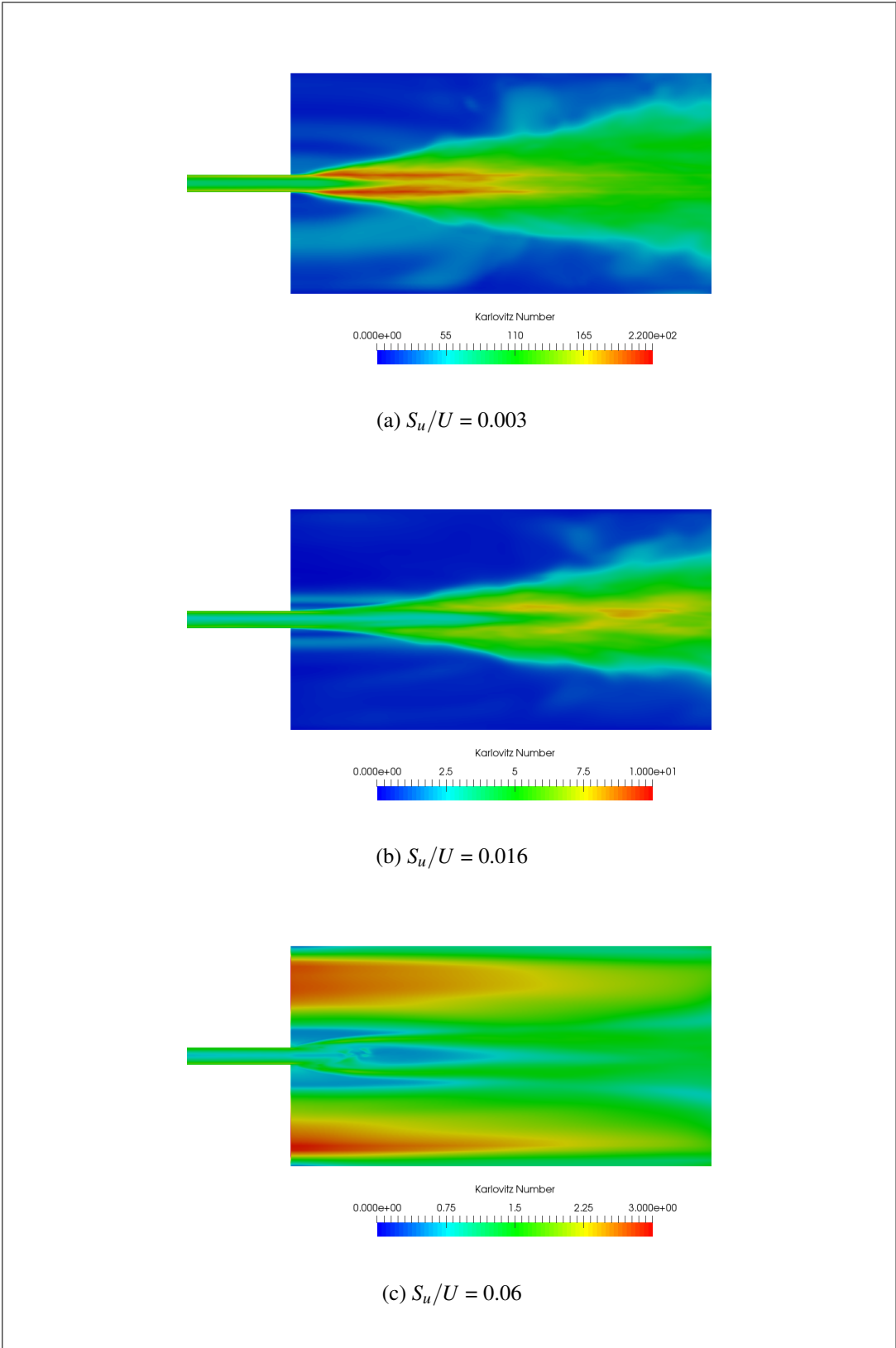


Figure 4.9: Time averaged Karlovitz numbers for different S_u/U configurations

Due to the 3D nature of the turbulent structures, it is easier to observe the wrinkling behavior in 3D views of the progress variable field. Therefore, a volume rendering of the instantaneous flame structure is presented in Figure 4.10.

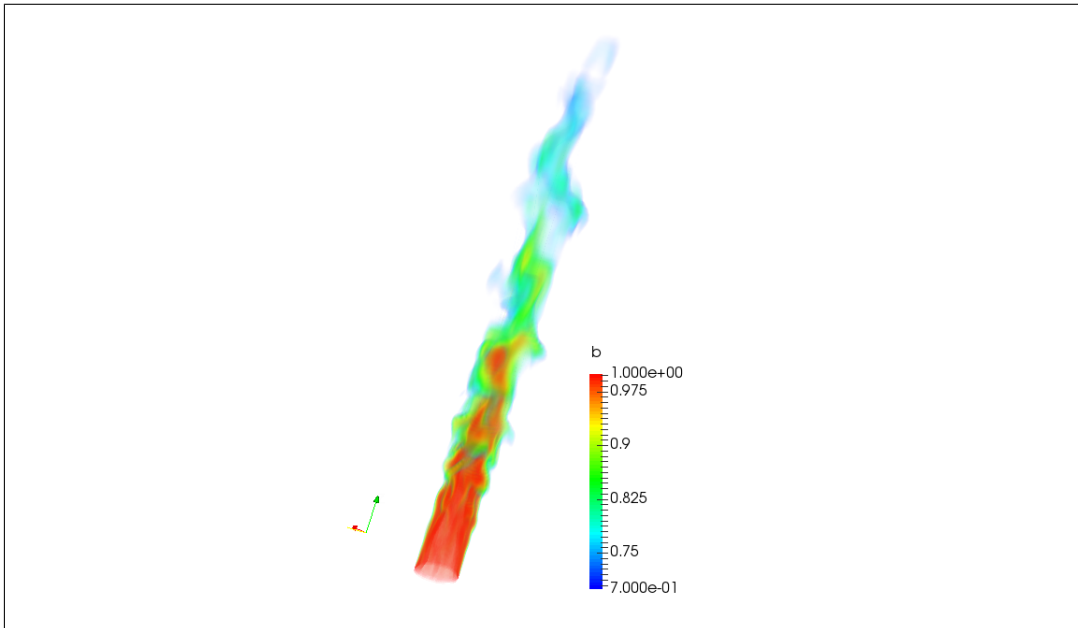


Figure 4.10: Volume rendering of instantaneous flame profile

Although no change in boundary conditions is made for the 3D simulation, it is important to note that by utilizing LES turbulence model, modeled sub-grid turbulent scales are taken into account when calculating the Ξ . This indicates that Equation 3.19 can be utilized for different premixed combustion configurations than the one in Bunsen burners, and this equation does not solely applicable on simplified 2D geometries or RANS turbulence model.

Gradient of the progress variable scalar can also be examined to get information on the flame wrinkling phenomenon. Since the gradient will have non-zero values for regions where transition from burned to unburned occur, it would be easier to observe wrinkling behavior. Instantaneous gradient fields for progress variable along with resolved turbulence intensity values are given in Figure 4.11. As seen, while cases b and c show flat flame surface behavior due to low turbulence intensity, wrinkling phenomenon can be clearly observed in case a, where turbulence intensity is higher than the other two.

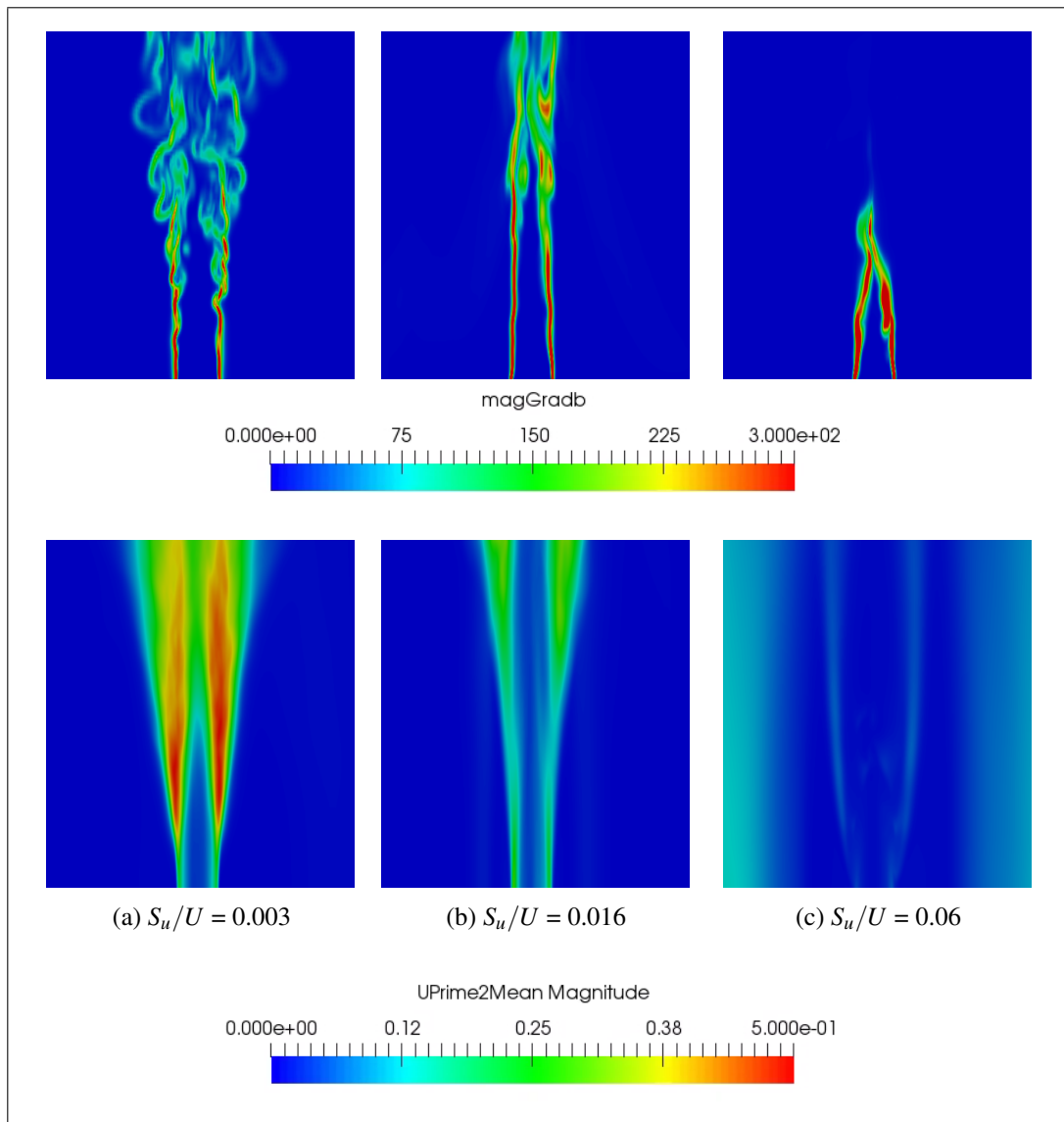


Figure 4.11: Gradient of instantaneous progress variable field and instantaneous velocity profiles for different S_u/U configurations

4.3 3D Backward Facing Step

After the validation of Equation 3.19 on the OpenFOAM framework with LES turbulence modeling approach, backward facing step with reacting flow is selected as a more complex and challenging case to further test the reaction closure equation performance. The non-reactive cold flow ($\phi = 0$) and the reacting propane combustion flow ($\phi = 0.57$) are simulated with the initial conditions of $p = 1$ atm, $T = 300$ K and $Re = 22,000$. Time averaged non-reactive velocity fields are compared to the experimental results in order to validate the numerical schemes, mesh and boundary conditions used in the simulation. Then, reactive flow is simulated using the same conditions and results are presented.

Figure 4.12 shows the streamwise velocity fields for the developed cold flow. The turbulent flow structures in Figure 4.12a are obtained after the flow has passed through the domain approximately five times. After this instantaneous field is obtained, flow is simulated for 9-10 more passes while taking the time average of velocity field, totaling up to an average simulation time of 1 second. Resulting time averaged velocity field is presented in Figure 4.12b. Both instantaneous and time averaged streamwise velocity profiles show that the flow is turbulent. The reason for the rise of turbulent structures in the early stages of the simulation is the mapped inlet boundary condition used in the simulation. A cross section 150 mm away from the inlet in the streamwise direction is selected and the flow is mapped from this section back to the inlet to create an infinitely long channel entry. With the help of this feature, breaking of the flow into turbulence is accomplished much more easily.

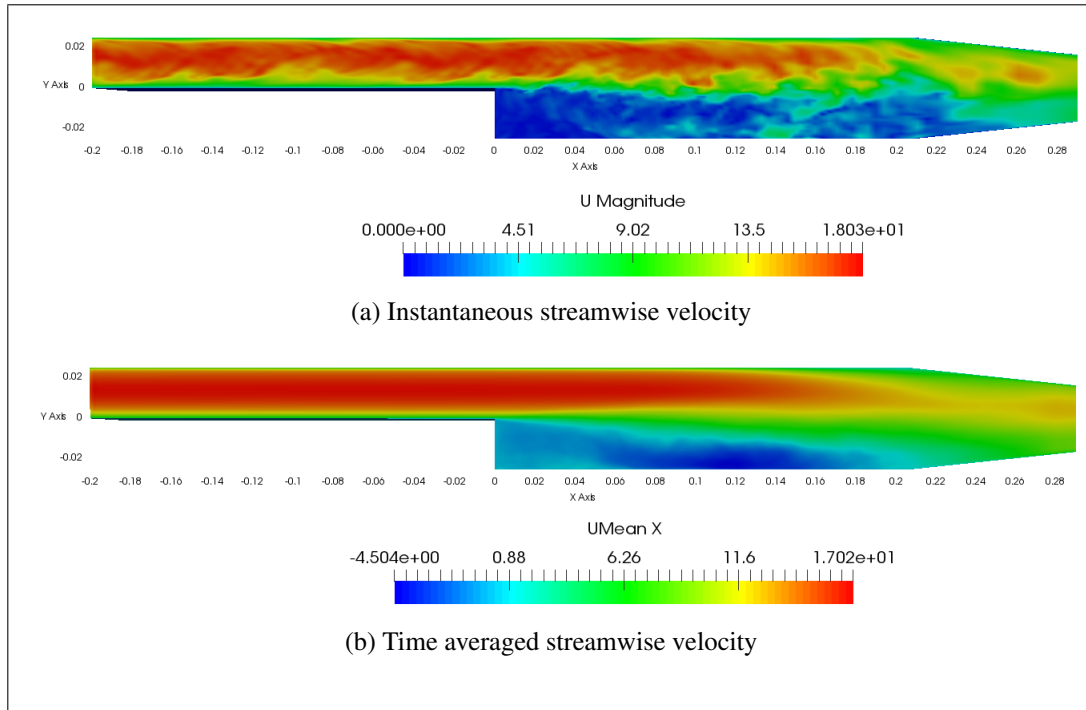


Figure 4.12: Streamwise velocity profiles for cold flow

In order to validate the flow field obtained from cold flow simulations, time averaged mean and fluctuating (root mean squared) velocity profiles for different cross sections are plotted and presented in Figures 4.13 and 4.14, respectively. Experimental and simulation data obtained from Weller [53] and Pitz & Daily [58] are used as a reference to compare the results. For normalizing the velocity, the inlet velocity $u_0 = 13.3$ m/s is used. Results obtained from the simulation are consistent with the experimental and simulation data, which validates the suitability of the computational grid, numerical schemes and boundary conditions used in the simulation. The deviations from the experimental data are expected, since the reference data was only available in the normalized form, amplifying the deviation visually. This discrepancy can be seen more clearly in Figure 4.14. However, the maximum deviation from the experimental results is around 5%, which is within an acceptable range.

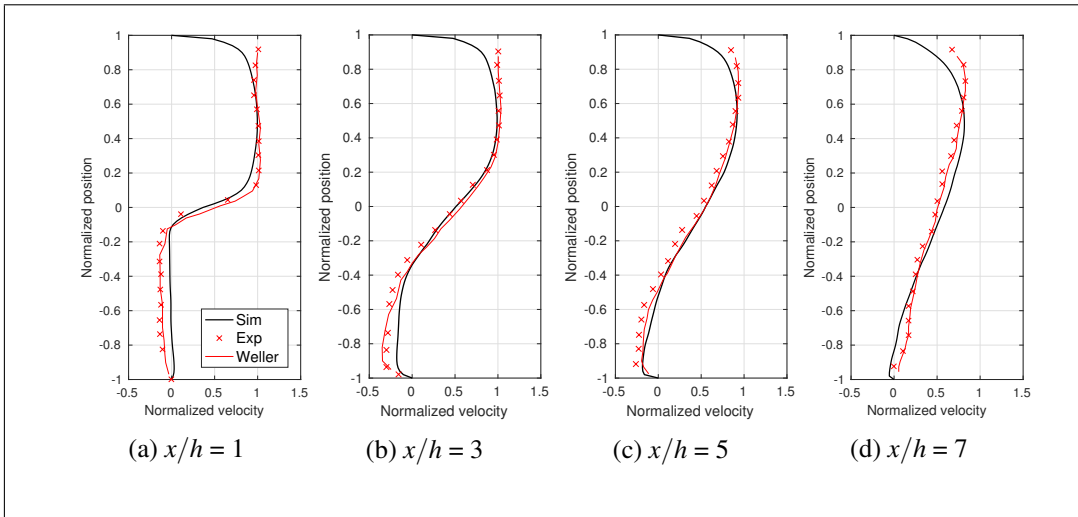


Figure 4.13: Time averaged profiles for streamwise velocity component at different cross sections for non-reacting flow

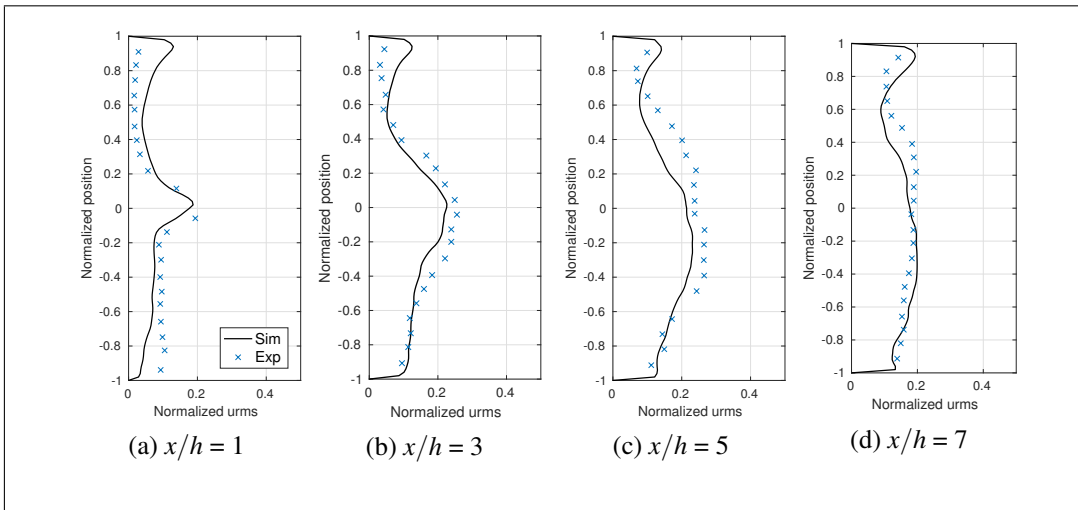


Figure 4.14: Time averaged profiles for streamwise velocity fluctuations at different cross sections for non-reacting flow

In the next step, reactive flow simulations are carried out. The non-reactive developed flow profiles are used as initial flow conditions and the reaction is initiated into the fully developed flow. Thermophysical properties are obtained from 1D Cantera simulations and given as initial conditions. In order to optimize the ignition process, the progress variable field is initialized by setting the step wall below the nozzle outlet to 0 and the field is developed from this boundary, as seen in Figure 4.15 [59].

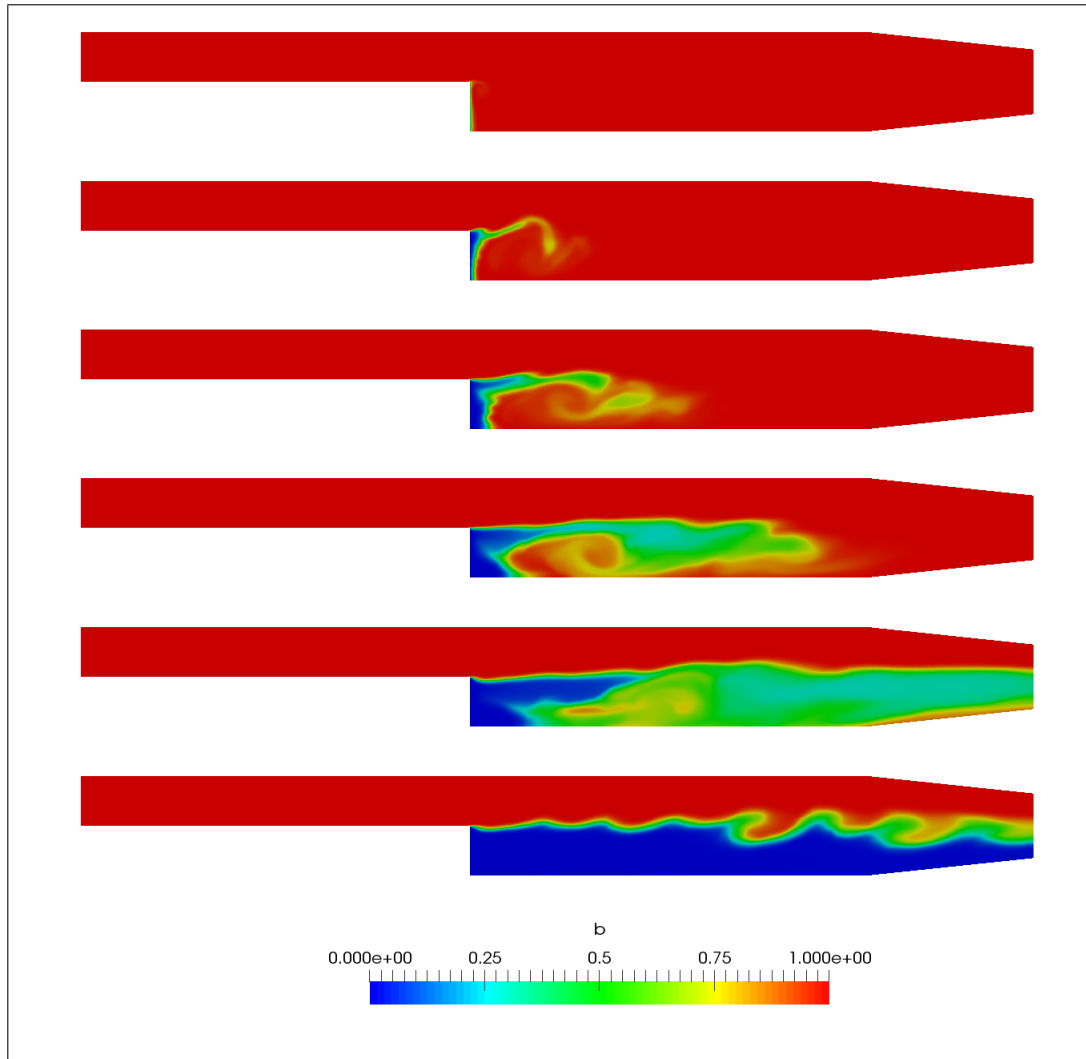


Figure 4.15: Instantaneous progress variable profiles for $t = 0$ to $t = 0.5$ s

Table4.2: Cantera initial conditions for $p = 1$ atm $\phi = 0.57$

	Temperature (K)	Density (kg/m ³)	Kinematic Viscosity (m ² /s)
Unburned	293	1.23	1.78e-05
Burned	1644.85	0.21	5.83e-05

As mentioned in the previous chapter, thermophysical properties are coupled with the progress variable field. The burned and unburned values of density and temperature are assigned to those regions directly from the ideal gas equation and Cantera initial conditions, which are listed in Table 4.2. The thermophysical properties of the flame region where progress variable is between 0 and 1 is linearly interpolated using burned

and unburned values. Since these values most likely do not show linear behavior inside a real flame, this approximation is one major drawback for the accuracy of progress variable approach. Instantaneous profiles of density and temperature with the corresponding progress variable field is given in Figure 4.16. As can be seen in the figure, density and temperature are perfectly correlated with the progress variable field and inside the physical range of the case.

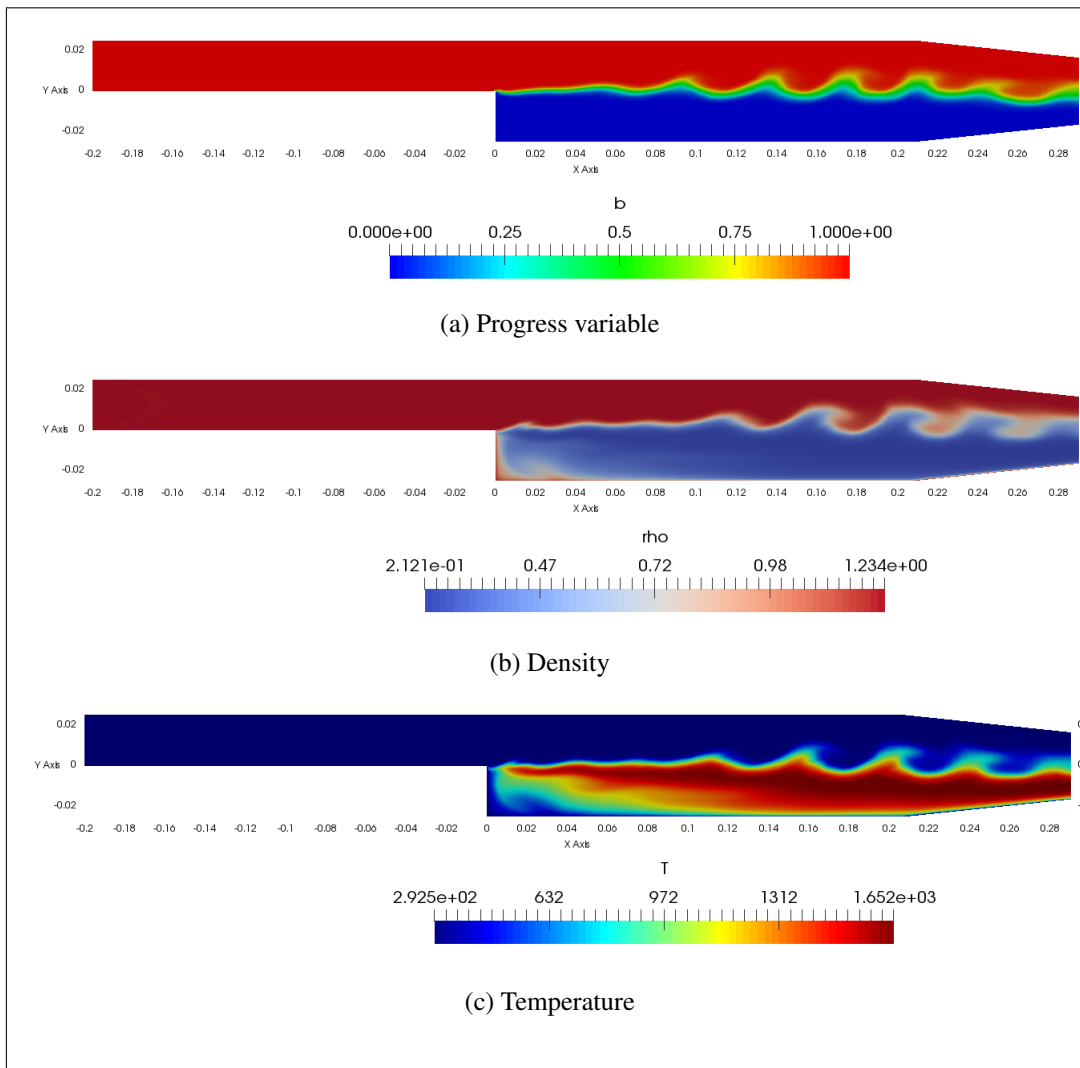


Figure 4.16: Thermodynamic parameters and progress variable fields

In the experiment, instantaneous profiles for the reactive flow is captured using Schlieren images, as seen in Figure 4.17 [53]. Comparing this image with the fully developed instantaneous profile in Figure 4.15 shows that the flame layer looks like a Kelvin-

Helmholtz instability profile rather than a straight line. This confirms that the approach is successful for modeling flame wrinkling.



Figure 4.17: Schlieren photograph of the reactive flow [53]

After the flow is completely developed, time averaged progress variable field is obtained by collecting the data for an extra 0.5 seconds as seen in Figure 4.18. In addition, gradient of the time averaged progress variable field is represented in Figure 4.19. From the change rate of progress variable it can be observed that flame is defined in a thin region between burned and unburned regions as expected. Post-processing analysis revealed that the thickness of the flame is around 5 mm and average filter size inside is around 1 mm, which are too coarse for obtaining inner flame structures.

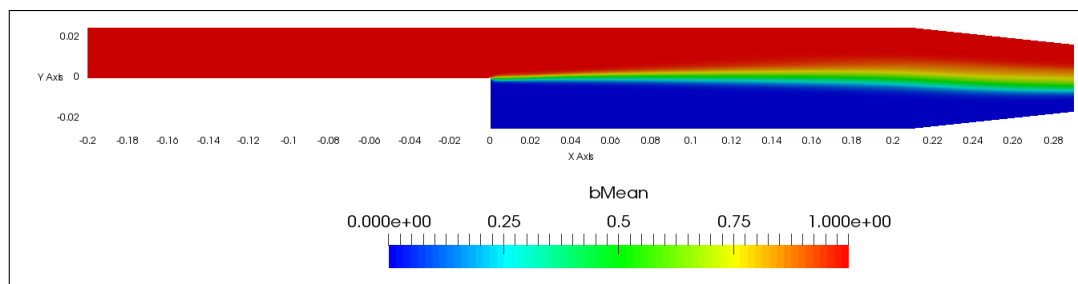


Figure 4.18: Time averaged progress variable field

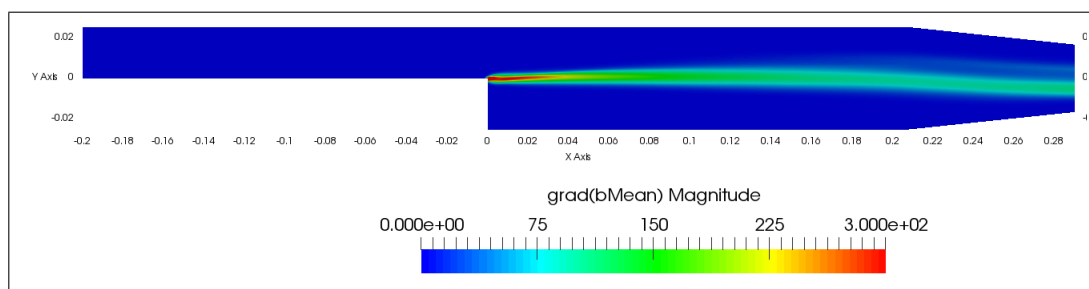


Figure 4.19: Gradient of time averaged progress variable field

Obtained time averaged field is also spatially averaged in the spanwise direction and

the resulting progress variable field is compared to the experimental results by using different cross sectional profiles in Figure 4.20. The experimental data used to compare with the progress variable is the normalized mass fraction of CO_2 at different cross sections. CO_2 emission is a chemically dominated phenomena and strongly depends on the chemical reactions inside the flame region. Therefore, the progress variable field is not consistent with the actual CO_2 mass fraction data inside the reaction zone. This inconsistency occurs since in progress variable approach, the chemical structures within the flame is completely ignored and parameters are linearly interpolated using burned and unburned properties. As a result, although the progress variable field fails to match the CO_2 emission results in the flame region, it captures the location of the flame in the domain. For example, in Figure 4.20b, the starting point of progress variable transition at 1 occurs around the position where CO_2 emission starts. This clearly indicates that while the proposed method can not resolve the region inside the flame, the boundaries of different regions of the premixed flame is captured by the progress variable.

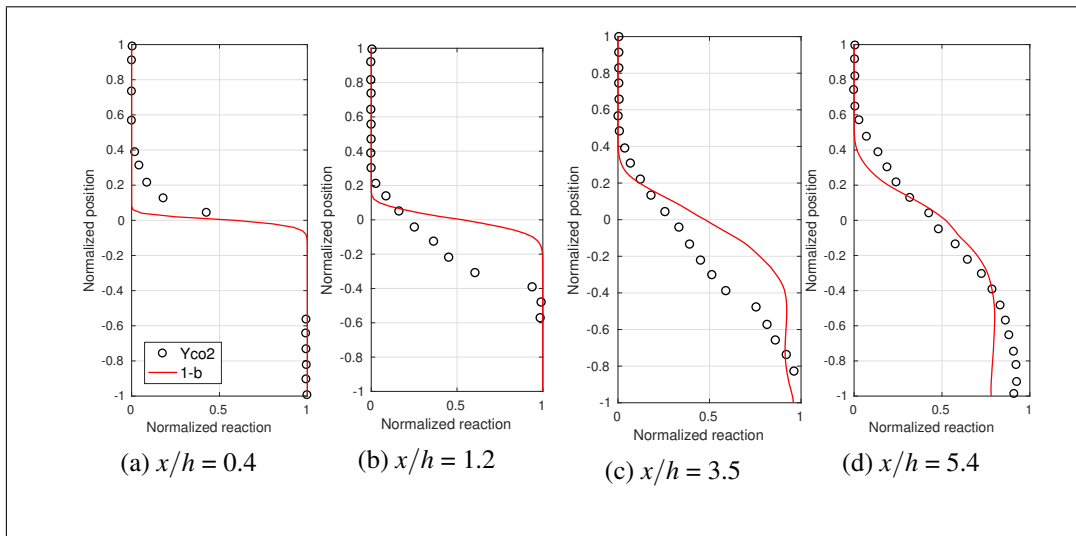


Figure 4.20: Time averaged profiles for progress variable values at different cross sections for reacting flow

One other feature of both reactive and non-reactive flows that can be investigated to validate the accuracy of the results is the reattachment (or re-circulation) length. Reattachment length is defined as the distance from the step wall to the position where flow reattaches to the wall [61]. Reattachment length can be found by plotting the wall shear stress and locating the position with the sign change. It can also be visually determined by examining streamline profiles of the flow field. Reattachment lengths measured from streamlines in Figures 4.21 and 4.22 are presented in Table 4.3 along with the experimental and simulation results for comparison. The experimental data is accurate in $\pm 0.5h$ interval, which makes the results within the acceptable range.

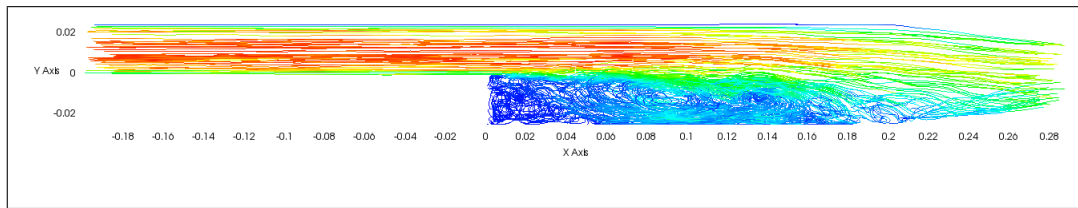


Figure 4.21: Streamlines for cold flow

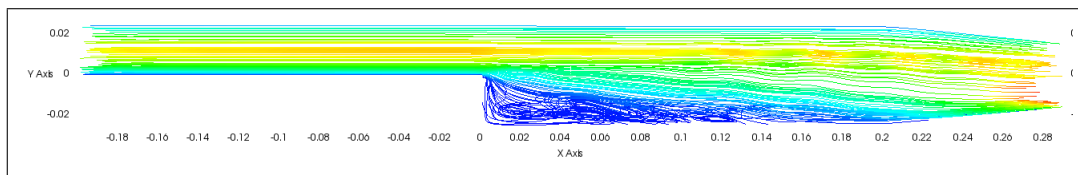


Figure 4.22: Streamlines for reactive flow

Table 4.3: Reattachment lengths for experiment and current simulation ($Re = 22,000$)

	Non-Reactive x/h	Reactive x/h
LES [59]	6.8	4.4
Experiment [58]	7.0	4.5
Current Results	7.08	4.7

4.3.1 Resolution of the Case in LES Modeling

The main idea behind LES turbulence model is to resolve the flow field as detailed as possible. Although generated results show good correlation with the experiments, determining the quantity of the resolved flow field is also important. Therefore, two

different parameters are calculated throughout the computational domain to further validate the results.

Two parameters important in assessing the quality of the LES simulation are integral length scale and Kolmogorov length scale. Integral length scale is a parameter describing the size of the large-eddy containing eddies in turbulent flows. Using turbulence parameters, it can be described as:

$$\ell = k^{3/2}/\varepsilon \quad (4.2)$$

For capturing the small scales, ratio of cubic root of the cell volume to this value should be less than around 0.08 [62]. In addition, one other parameter for assessing the LES performance is the Kolmogorov length scale, which is defined as:

$$\eta = (v^3/\varepsilon)^{1/4} \quad (4.3)$$

For DNS applications, ratio of cubic root of the cell volume to the Kolmogorov length scale should be around 1 to 3. For LES applications, this value should be less than 10 [63].

In the light of this information, following two conditions should be satisfied by the computational simulation to successfully capture the small scale turbulence:

$$\begin{aligned} \frac{V^{1/3}}{k^{3/2}/\varepsilon} &< 0.08 \\ \frac{V^{1/3}}{(v^3/\varepsilon)^{1/4}} &< 10 \end{aligned} \quad (4.4)$$

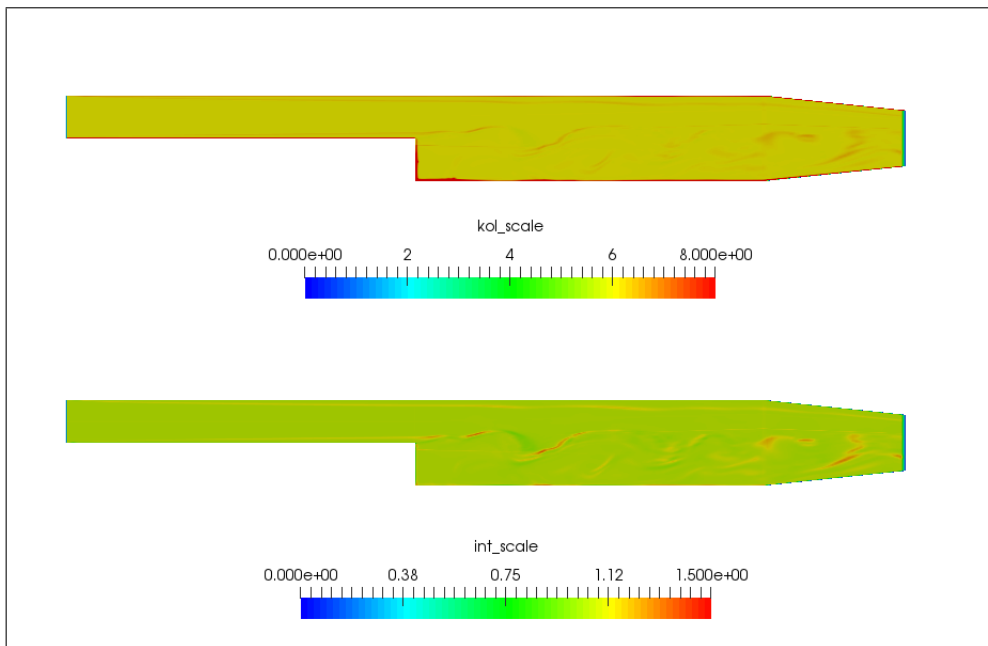


Figure 4.23: Kolmogorov and integral length scale contours

For the backward facing step simulation, contour plots of these quantities are given in Figure 4.23. The results show that, although the condition for the Kolmogorov length scale is satisfied, cell size to integral length scale ratio is above the desired threshold. Although this affects the amount of resolved eddies in the simulation, behavior of the flame front is not heavily affected since the reaction region where chemistry takes place is already filtered out by the computational grid. Having a coarse mesh would result with a thickened flame but the behavior of that flame front will not be affected.

4.4 Discussion

Both Bunsen burner and backward facing step cases show that the progress variable approach using the rate closure term in Equation 3.19 is successful in capturing flow and thermophysical characteristics of each case. Although small deviations are seen from the experimental data, considering both the numerical deviations arise from CFD side such as round-off errors, numerical diffusivity, turbulence modeling and the typical error margins in any experiment, it is safe to say that the results are quite satisfactory within the acceptable range.

Firstly, results of performed Cantera simulations for free flames conform experimental results of reactive flows. This is a crucial step, since these results are directly given as initial conditions for burned and unburned regions explicitly. As chemical reactions are not resolved when using the progress variable approach, getting the initial conditions by simplified Cantera analysis with detailed chemistry approach is quite important. In all simulations, thermophysical properties of the burned and unburned regions are consistent with the available experimental data.

2D Bunsen burner simulations after implementing Equation 3.19 reveal that if appropriate rate modeling is used, the approach is successful for capturing the flame position and thermophysical properties for both burned and unburned regions. Preliminary analysis performed by sweeping the pressure and equivalence ratios while keeping all other parameters constant shows that the model reacts to change in the thermophysical properties as it is expected. While the increased pressure results in higher turbulent flame speed and smaller Bunsen cone, change in the equivalence ratio directly affects the laminar flame speed. In addition, it also causes change in the flame cone is correlated with the laminar flame speed - equivalence ratio relation, presented in Figure 3.3. It is important that the turbulent flame speed is sensitive to the changes in thermophysical properties during the simulations, considering that chemistry and thermodynamics are not resolved by the proposed approach. This preliminary analysis ensures that although explicitly defined, thermophysical aspect of the combustion process is still taken into account.

Three propane flames that are simulated and compared with the experimental data

using normalized flame angles show that the time averaged progress variable fields are quite consistent with the experimental Bunsen flames. Since Equation 3.19 is derived by fitting a function into experimental Bunsen flame, correlation in results is expected. Some approximations are made for defining burned and unburned regions properly, since the flame region is not infinitely thin due to numerical dissipation in the scalar transport equation. The reason for this dissipation comes from the discretization and numerical schemes used for increased stability. Although the approach states that the burned region is represented by the value 0, b value ranging from 1-0.9 is selected for unburned representation, thus assuming a region is burned when b is smaller than 0.9. By using this assumption, flame shapes are compared in Figure 4.4. The obtained flame shapes fits to the results gathered from the experimental setup.

3D analysis of the selected Bunsen flame can be considered as an intermediate step linking this analysis of the backward step to the 2D Bunsen burner validation cases. Simulations performed with different S_u show that according to the position of the case in the Borghi diagram, different premixed flame characteristics can be observed. While more turbulent configurations would result with wrinkled flames and blow-off phenomena, increasing the laminar flame speed enables the flame to dominate over turbulent effects and flatten out the wrinkles. By increasing this sufficiently so that the process is in laminar flamelet region, steady profiles such as Bunsen cone can be obtained.

Cold flow analysis results for the backward facing step are consistent with experimental results and give insight about the complexity of the case. The high Reynolds number of the case requires highly resolved shear layer region, which needs high resolution near the walls. Although average $y^+ < 1$ condition is satisfied for all wall boundaries, refining the mesh near shear layer regions may result in more correlated results with the experiment. Furthermore, wall functions for turbulence parameters can be utilized to enhance the accuracy. Results presented in Figure 4.13 and 4.14 show that the accuracy is good enough even with current configuration.

During the course of running the simulations, different initialization approaches for the reactive case were investigated. By default, OpenFOAM uses ignition approach by setting a certain region defined by the user to burned gradually over the prescribed

time. However, pressure waves and high velocity gradients arise when this method is not optimized properly. This is a tedious work, since every single case requires a specific ignition initial condition by trial and error. To prevent that, setting one of the relevant boundaries to burned condition and the progress of the flame from that boundary by convection is preferred.

When assessing the performance of the approach in the backward facing step, different parameters are used. Firstly, the instantaneous progress variable fields obtained from the spanwise centerline surface shows that the flame wrinkling phenomena is captured properly by the proposed approach. Comparing the instantaneous profiles with Schlieren photograph of the reactive flow in Figure 4.17 also shows a general similarity in flow behavior and flame wrinkling positions. Considering the computational cost of modeling the combustion flame using a detailed chemistry approach, obtaining the wrinkling behavior by solving only a single scalar transport equation can be considered as an achievement for extending this modeling approach to industrial combustion problems. Furthermore, solving a reactive case with such high Reynolds number and turbulent behavior using detailed chemistry is almost impossible with the current computational power available for industrial or academic applications.

Time averaged progress variable profiles for different cross sections of the backward facing step and normalized CO_2 mass fraction results show strong correlations as seen in Figure 4.20. As mentioned in the previous chapter, progress variable method utilizes a global one step chemistry approach which only accounts for fully burned and unburned states of the combustion.

CHAPTER 5

CONCLUSION

5.1 Summary and Overview

In this thesis, accuracy of the progress variable approach for simulating premixed combustion process was investigated. The source term, which includes the effect of the chemistry and flow onto the flame shape, was modeled using model equation from literature and implemented into the OpenFOAM framework. Different features of OpenFOAM and Cantera were used for pre-processing and simulation steps. Post-processing is performed in ParaView, an open source, multi-platform data analysis and visualization tool [64].

After the implementation of the new source term relation to OpenFOAM, the performance of the new solver was validated through 2D Bunsen burner simulations. Different Bunsen burner flames were simulated to show the sensitivity of the solver to changes in the thermophysical and flow properties. Obtained flame shape profiles and non-dimensionalized flame angles were compared with the experimental flame results to prove that both the approach and the implemented source term relation are successful in capturing premixed combustion process. With validating the performance by both visual inspection of the flame shapes and the non-dimensionalized flame angles, simulations were extended into 3D. A 3D computational grid for the same burner with same inlet geometry and boundary conditions was constructed, and the performance of the source term relation in simulations with LES turbulence modeling was verified. Ability of the solver in capturing stretching and wrinkling effects was validated.

Since a quasi-steady application such as Bunsen burner was not sufficient to verify

the applicability of the model completely, reactive backward facing step flow with Reynolds number of 22,000 was also simulated to validate the closure rate equation for turbulent flows. In non-reactive flow analysis, averaged fields of mean and fluctuating velocity showed good agreement with the experimental results. In reactive case the approach managed to get a good result about the position of the flame front inside the domain. It also managed to capture the wrinkling behavior of the flame layer during the process.

5.2 Review of the Thesis Objectives

In Chapter 1, objectives for the thesis were set. These objectives are presented below again to comment on how well they were accomplished throughout the thesis.

1. Implementation of an existing source term reaction closure equation from literature to the OpenFOAM progress variable solver
 - For modeling chemical and turbulent effects onto the flame, a source term equation derived from the experimental Bunsen flame data was implemented to the OpenFOAM framework. Information on both new equation and default OpenFOAM equation was given. By implementing this algebraic source term definition into OpenFOAM framework, an improved version of the progress variable solver made available for the OpenFOAM user community.
2. 2D Bunsen burner flame analysis with the RANS turbulence model and comparison with experimental results
 - Preliminary analysis performed with different pressure and equivalence ratio configurations proved that the model behaves as expected to the changes in the thermophysical or ambient properties.
 - Both flame shape and non-dimensionalized flame angle results of the simulations were consistent with the experimental profiles.
3. Extension of the 2D RANS Bunsen burner analysis to 3D LES simulations and verifying the applicability of the source term in LES

- 3D analysis of the Bunsen flame gave similar results with the 2D configuration.
 - Calculation of turbulence properties from the LES model validated the applicability of the model to LES simulations.
 - The method managed to capture flame stretching and wrinkling effects in the wrinkled and corrugated regions properly.
4. 3D backward facing step simulation to show the performance of the model in the turbulent reactive flow
- Simulation of a non-reactive flow showed good correlation with the experimental results. Both time averaged mean streamwise velocity and streamwise velocity fluctuations fit the experimental profiles nicely, thus validating the used mesh, numerical schemes and boundary conditions.
 - Reactive profiles obtained by the time averaged progress variable field managed to capture the flame front position in the domain. By the nature of the approach, no information was obtained on the mass fractions of chemical species involved in combustion.

As mentioned before, the progress variable approach requires well defined simulation cases with appropriate physical and numerical properties. Although the objectives set at the beginning of the thesis were mostly satisfied, there is still room for improvement and corrections. A table giving the information on achieved goals along with some pitfalls and suggestions is given in Figure 5.1.

5.3 Future Work

In addition to the work performed throughout this thesis, more studies can be conducted to further investigate and improve the premixed combustion simulations. Some key points are summarized below.

- Although average $y^+ < 1$ is satisfied for backward facing step, computational grid can be refined more to resolve smaller turbulent scales, which in turn increases the accuracy of the solution.

- Schemes with limiter characteristics and numerical dissipation are used for progress variable parameters to enhance the stability. By trying out different computational grids and numerical schemes, less dissipative schemes can be used to resolve the flame and better estimation for its position.
- Since progress variable assumes one step global reaction, the chemistry inside the flame is completely ignored. This can be improved by introducing small mechanisms (3-7 steps) to the solver in order to partially resolve the chemistry inside the reaction zone.
- Other approaches such as Direct Chemistry Method or FGM method can be utilized in the same simulation cases to compare their performance with the progress variable approach.
- Other premixed combustion applications with available reference data can be simulated to further verify the solver and its benchmark abilities.
- Instead of using constant enthalpy approach, thermodynamic polynomials and Sutherland formulation can be used to calculate the enthalpy and kinematic viscosity in the simulations. Although the chemistry will still remain unresolved, this approach might give more accurate detail inside the reaction zone.

Case	What has been achieved	Problems / Pitfalls	Improvements / Suggestions
2D Bunsen Burner	<ul style="list-style-type: none"> Results similar to experimental flame profiles obtained. Non-dimensional flame angles agree with experiments. 	<ul style="list-style-type: none"> Boundary conditions, especially outlet, was problematic. Unwanted pseudo pressure waves created at the outlet and distorted the solution. Second order time schemes gave unreasonable inlet flow profiles. 	<ul style="list-style-type: none"> All scalars at the outlet were set to Neumann boundary condition. Pressure boundary condition at the outlet selected as pressure transmissive. Therefore, waves are transferred out of the domain instead of bouncing back. The simulation run with Euler time scheme for ~500 steps then switched to second order.
3D Bunsen Burner	<ul style="list-style-type: none"> Similar results to 2D case is obtained. Validation of the model in 3D LES simulations is achieved. 	<ul style="list-style-type: none"> Ignition phase was problematic by setting the outlet boundary to burned. 	<ul style="list-style-type: none"> Instead of only setting the outlet boundary to burned, half of the domain is set as burned with proper temperature and progress variable as an initial condition.
3D Backward Facing Step	<ul style="list-style-type: none"> Good agreement with experimental velocity profiles obtained. Flame front position and flame wrinkling captured correctly. Validation of the model in a turbulent flow is achieved. 	<ul style="list-style-type: none"> Obtaining developed turbulent profile took long time in non-reacting flow. Deciding on the duration of time averaging was trial and error. Progress variable was not able to capture the trends inside the flame. 	<ul style="list-style-type: none"> Turbulent structures can be obtained much faster by introducing perturbations at the inlet using "perturbU" utility of OpenFOAM. After the developed profile observed visually, flow should past the domain 2-3 times more, then averaging should be performed twice that time. Instead of using a single step global reaction approach, small mechanisms of 2-3 steps can be introduced to the code to increase the chemical accuracy of the solution in a FGM-like approach.

Figure 5.1: Review table for performed simulations

REFERENCES

- [1] J Warnatz, U Maas, and R W Dibble. *Combustion : Physical and Chemical Fundamentals, Modelling and Simulation, Experiments, Pollutant Formation*. Springer, 1999. ISBN:978-3-540-45363-5.
- [2] Pierre Sagaut. *Large eddy simulation for incompressible flows*. Springer, 1 edition, 2010. ISBN:978-3-540-26344-9.
- [3] Heinz Pitsch and By Heinz. Large-Eddy Simulation of Turbulent Combustion. *Annu. Rev. Fluid Mech*, 38:453–82, 2006. doi:10.1146/annurev.fluid.
- [4] K. Mahesh, G. Constantinescu, S. Apte, Gianluca Iaccarino, Frank Ham, and Parviz Moin. Large-eddy simulation of reacting turbulent flows in complex geometries. *Journal of Applied Mechanics*, 73(3):374, 2006. doi:10.1115/1.2179098.
- [5] I Langella, N Swaminathan, F A Williams, J Furukawa, and A Williams. Large-eddy simulation of premixed combustion in the corrugated-flamelet regime. *Combustion Science and Technology*, 188(9):1565–1591, 2016. doi:10.1080/00102202.2016.1195824.
- [6] Hideaki Kobayashi, Teppei Nakashima, Takashi Tamura, Kaoru Maruta, and Takashi Niioka. Turbulence Measurements and Observations of Turbulent Premixed Flames at Elevated Pressures up to 3.0 MPa. 1997. doi:10.1016/S0010-2180(96)00103-4.
- [7] T. J. Poinso and D. P. Veynante. *Encyclopedia of Computational Mechanics*. Wiley, 2004. ISBN:9780470091357.
- [8] D. Durox, S. Ducruix, and S. Candel. Experiments on collapsing cylindrical flames. *Combustion and Flame*, 125(1-2):982–1000, 2001. doi:10.1016/S0010-2180(00)00254-6.
- [9] U.S. Energy Information Administration (EIA). *International Energy Outlook 2016*. 2016. (visited on 24/05/2017).
- [10] Turkish Statistical Institute. http://www.turkstat.gov.tr/PreTablo.do?alt_id=1029, 2015. (visited on 20/05/2017).
- [11] Mustafa Servet Kiran, Eren Özceylan, Mesut Gündüz, and Turan Paksoy. Swarm intelligence approaches to estimate electricity energy demand in turkey. *Knowledge-Based Systems*, 36:93–103, 2012. doi:10.1016/j.knosys.2012.06.009.
- [12] U.S. Environmental Protection Agency. <https://www.epa.gov/no2-pollution>, 2017. (visited on 25/07/2017).

- [13] Imo global sulphur cap. <http://www.imo.org/en/mediacentre/pressbriefings/pages/mepc-70-2020sulphur.aspx>. [Online; accessed 2017/10/31].
- [14] Thierry Poinsot. Using direct numerical simulations to understand premixed turbulent combustion. *Symposium (International) on Combustion*, 26(1):219–232, 1996. doi:10.1016/S0082-0784(96)80220-7.
- [15] T. Ma, O. T. Stein, Nilanjan Chakraborty, and A. M. Kempf. A posteriori testing of algebraic flame surface density models for LES. *Combustion Theory and Modelling*, 17(3):431–482, 2013. doi:10.1080/13647830.2013.779388.
- [16] Christophe Duwig. A filtered flame approach for simulation of unsteady laminar premixed flames. *Combustion Theory and Modelling*, 13(2):251–268, 2009. doi:10.1080/13647830802578429.
- [17] Norbert Peters. *Turbulent Combustion*. Cambridge University Press, 2001. ISBN:978-0521660822.
- [18] E. R. Hawkes and R. S. Cant. Implications of a flame surface density approach to large eddy simulation of premixed turbulent combustion. *Combustion and Flame*, 126(3):1617–1629, 2001. doi:10.1016/S0010-2180(01)00273-5.
- [19] Norbert Peters. The turbulent burning velocity for large-scale and small-scale turbulence. *Journal of Fluid Mechanics*, 384:107–132, 1999. doi:10.1017/S0022112098004212.
- [20] CFD Online - Karlovitz number. https://www.cfd-online.com/Wiki/Karlovitz_number. (visited on 14/06/2017).
- [21] M. Ghaderi Masouleh, A. Wehrfritz, O. Kaario, H. Kahila, and V. Vuorinen. Comparative study on chemical kinetic schemes for dual-fuel combustion of n-dodecane/methane blends. *Fuel*, 191:62–76, 2017. doi:10.1016/j.fuel.2016.10.114.
- [22] S.M. Sarathy, C.K. Westbrook, M. Mehl, W.J. Pitz, C. Togbe, P. Dagaut, H. Wang, M.A. Oehlschlaeger, U. Niemann, K. Seshadri, P.S. Veloo, C. Ji, F.N. Egolfopoulos, and T. Lu. Comprehensive chemical kinetic modeling of the oxidation of 2-methylalkanes from {C7} to {C20}. *Combustion and Flame*, 158(12):2338 – 2357, 2011. doi:10.1016/j.combustflame.2011.05.007.
- [23] E. Ranzi, A. Frassoldati, R. Grana, A. Cuoci, T. Faravelli, A.P. Kelley, and C.K. Law. Hierarchical and comparative kinetic modeling of laminar flame speeds of hydrocarbon and oxygenated fuels. *Progress in Energy and Combustion Science*, 38(4):468 – 501, 2012. doi:10.1016/j.pecs.2012.03.004.
- [24] Krithika Narayanaswamy, Perrine Pepiot, and Heinz Pitsch. A chemical mechanism for low to high temperature oxidation of n-dodecane as a component of transportation fuel surrogates. *Combustion and Flame*, 161(4):866 – 884, 2014. doi:10.1016/j.combustflame.2013.10.012.
- [25] Eliseo Ranzi, Alessio Frassoldati, Alessandro Stagni, Matteo Pelucchi, Alberto Cuoci, and Tiziano Faravelli. Reduced kinetic schemes of complex reaction

- systems: Fossil and biomass-derived transportation fuels. *International Journal of Chemical Kinetics*, 46(9):512–542, 2014. doi:10.1002/kin.20867.
- [26] Zhaoyu Luo, Sibendu Som, S. Mani Sarathy, Max Plomer, William J. Pitz, Douglas E. Longman, and Tianfeng Lu. Development and validation of an n-dodecane skeletal mechanism for spray combustion applications. *Combustion Theory and Modelling*, 18(2):187–203, 2014. doi:10.1080/13647830.2013.872807.
- [27] J.A. Van Oijen and L.P.H. De Goey. Modelling of Premixed Laminar Flames using Flamelet-Generated Manifolds. *Combustion Science and Technology*, 161(1):113–137, 2000. doi:10.1080/00102200008935814.
- [28] GRI-Mech 3.0 Mechanism. <http://combustion.berkeley.edu/gri-mech/version30/text30.html>. (visited on 15/06/2017).
- [29] Alessio Fancello. *Dynamic and turbulent premixed combustion using Flamelet-Generated Manifold in OpenFOAM*. PhD thesis, 2017. doi:10.6100/IR781467.
- [30] Armin Wehrfritz, Ossi Kaario, Ville Vuorinen, and Bart Somers. Large Eddy Simulation of n-dodecane spray flames using Flamelet Generated Manifolds. *Combustion and Flame*, 167:113–131, 2016. doi:10.1016/j.combustflame.2016.02.019.
- [31] M. Dekena and N. Peters. Combustion modeling with the G-equation. *Oil and Gas Science and Technology*, 54(2):265–270, 1999. doi:10.2516/ogst:1999024.
- [32] Heinz Pitsch and L. Duchamp de Lageneste. Large-eddy simulation of premixed turbulent combustion using a level-set approach. *Proceedings of the Combustion Institute*, 29(2):2001–2008, 2002. doi:10.1016/S1540-7489(02)80244-9.
- [33] Heinz Pitsch. A G-equation formulation for large-eddy simulation of premixed turbulent combustion. *Center for Turbulence Research Annual Research Briefs*, pages 4–7, 2002.
- [34] L Duchamp de Lageneste and Heinz Pitsch. A level-set approach to large eddy simulation of premixed turbulent combustion. Technical report, 2000.
- [35] Libby P.A. Bray, K.N.C. and Moss J.B. Unified modelling approach for premixed turbulent combustion- part i : General formulation. *Combustion Flame*, 61:87–102, 1985. doi:10.1016/0010-2180(85)90075-6.
- [36] Wen Lin. Large-Eddy Simulation of Premixed Turbulent Combustion Using Flame Surface Density Approach. *University of Toronto*, 2010.
- [37] S. P. Reddy Muppala, Naresh K. Aluri, Friedrich Dinkelacker, and Alfred Leipertz. Development of an algebraic reaction rate closure for the numerical calculation of turbulent premixed methane, ethylene, and propane/air flames for pressures up to 1.0 MPa. *Combustion and Flame*, 140(4):257–266, 2005. doi:10.1016/j.combustflame.2004.11.005.

- [38] N K Aluri, S Muppala, and F Dinkelacker. Large-eddy simulation of lean premixed turbulent flames of three different combustion configurations using a novel reaction closure. *Flow, Turbulence and Combustion*, 80(2):207–224, 2008. doi:10.1007/s10494-007-9114-2.
- [39] Nasim Shahbazian. Comparative Study of Algebraic and Transported FSD Models for LES of Premixed Flames in Flamelet and Thin Reaction Zone Regimes. (January):326–331, 2012. doi:10.2514/6.2013-1138.
- [40] Ehsan Yasari. *Extension of OpenFOAM Library for RANS Simulation of Premixed Turbulent Combustion*. PhD thesis, 2013.
- [41] P D Nguyen, P Bruel, and S Reichstadt. An experimental database for benchmarking simulations of turbulent premixed reacting flows: Lean extinction limits and velocity field measurements in a dump combustor. *Flow, Turbulence and Combustion*, 82(2):155–183, 2009. doi:10.1007/s10494-008-9160-4.
- [42] LTT Erlangen Combustion Technology lecture notes. http://staatsmacht.org/Veranstaltungen/Verbrennungstechnik/Exercise4_CT.pdf. (visited on 01/07/2017).
- [43] H.K: Versteeg and W. Malalasekera. *An Introduction to Computational Fluid Dynamics - The Finite Volume Method*. 1995. ISBN:0-470-23515-2.
- [44] H. G. Weller, G. Tabor, H. Jasak, and C. Fureby. A tensorial approach to computational continuum mechanics using object-oriented techniques. *Computers in Physics*, 12(6):620, 1998. doi:10.1063/1.168744.
- [45] Cantera Documentation. <http://www.cantera.org/docs/sphinx/html/index.html>. (visited on 15/06/2017).
- [46] Donald F. Young, Bruce R; Munson, Theodore H; Okiishi, and Wade W Huebsch. *A Brief Introduction to Fluid Mechanics*, volume 1. Wiley, 2015. ISBN:0471362433.
- [47] Compressible Navier Stokes Equations. https://math.la.asu.edu/~gardner/fluid_eqs.pdf. (visited on 07/08/2017).
- [48] Karri Keskinen, Mika Nuutinen, Ossi Kaario, Ville Vuorinen, Jann Koch, Yuri M. Wright, Martti Larmi, and Konstantinos Boulouchos. Hybrid LES/RANS with wall treatment in tangential and impinging flow configurations. *International Journal of Heat and Fluid Flow*, 65:1339–1351, 2017. doi:10.1016/j.ijheatfluidflow.2017.04.001.
- [49] V Vuorinen, A Chaudhari, and J. P. Keskinen. Large-eddy simulation in a complex hill terrain enabled by a compact fractional step OpenFOAM?? solver. *Advances in Engineering Software*, 79:70–80, 2015. doi:10.1016/j.advensoft.2014.09.008.
- [50] Ehsan Yasari. Tutorial XiFoam. http://http://www.tfd.chalmers.se/~hani/kurser/0S_CFD_2010/ehsanYasari/ehsanYasariReport.pdf, 2010.

- [51] K. N. C. Bray and P. A. Libby. Recent developments in the BML model of premixed turbulent combustion. *Turbulent Reacting Flows*, (47):253–274, 1994.
- [52] M. Boger, D. Veynante, H. Boughanem, and A. Trouvé. Direct numerical simulation analysis of flame surface density concept for large eddy simulation of turbulent premixed combustion. *Symposium (International) on Combustion*, 27(1):917 – 925, 1998. doi:10.1016/S0082-0784(98)80489-X.
- [53] H.G. Weller, G Tabor, A.D. Gosman, and C Fureby. Application of a flame-wrinkling LES combustion model to a turbulent mixing layer. *Symposium (International) on Combustion*, 27(1):899–907, 1998. doi:10.1016/S0082-0784(98)80487-6.
- [54] G Tabor and H G Weller. Large eddy simulation of premixed turbulent combustion using flame surface wrinkling model. 72:1–28, 2004. doi:10.1023/B:APPL.0000014910.06345.fb.
- [55] OpenFoam Bug Report on XiFoam. <https://bugs.openfoam.org/view.php?id=311>. (visited on 13/07/2017).
- [56] William Lowry, Jaap de Vries, Michael Krejci, Eric Petersen, Zeynep Serinyel, Wayne Metcalfe, Henry Curran, and Gilles Bourque. Laminar flame speed measurements and modeling of pure alkanes and alkane blends at elevated pressures. *Journal of Engineering for Gas Turbines and Power*, 133(9):091501, 2011. doi:10.1115/1.4002809.
- [57] Ömer L. Gülder. Correlations of laminar combustion data for alternative s.i. engine fuels. In *SAE Technical Paper*. SAE International, 1984. doi:10.4271/841000.
- [58] R. W. Pitz and J. W. Daily. Combustion in a turbulent mixing layer formed at a rearward-facing step. *AIAA Journal*, 21(11):1565–1570, 1983. doi:10.2514/3.8290.
- [59] Nam Seob Park and Sang Cheol Ko. Large eddy simulation of turbulent premixed combustion flows over backward facing step. *Journal of Mechanical Science and Technology*, 25(3):713–719, 2011. doi:10.1007/s12206-011-0106-8.
- [60] Heinz Pitsch. Lecture notes in Combustion Theory, July 2014.
- [61] Michal A Kopera, Robert M Kerr, Hugh M Blackburn, and Dwight Barkley. Direct numerical simulation of turbulent flow over a backward-facing step. 2014. doi:10.1017/S0022112096003941.
- [62] The negatively buoyant wall-jet: Les results. *International Journal of Heat and Fluid Flow*, 25(5):795 – 808, 2004. Selected papers from the 4th International Symposium on Turbulence Heat and Mass Transfer.
- [63] H. Aref and S. Balachandar. *A First Course in Computational Fluid Dynamics*. Cambridge University Press, 2017.
- [64] Paraview. <https://www.paraview.org/>. (visited on 11/07/2017).